UNIVERSITY OF OKLAHOMA

GRADUATE COLLEGE

ADSORPTIVE TRAPPING OF BIO-OIL COMPOUNDS ONTO ACTIVATED CARBON

A THESIS

SUBMITTED TO THE GRADUATE FACULTY

in partial fulfillment of the requirements for the

Degree of

MASTER OF SCIENCE

By

ISSAC RAY SCHNEBERGER
Norman, Oklahoma
2016

ADSORPTIVE TRAPPING OF BIO-OIL COMPOUNDS ONTO ACTIVATED CARBON

A THESIS APPROVED FOR THE
SCHOOL OF CHEMICAL, BIOLOGICAL AND MATERIALS ENGINEERING

BY

_____
Dr. Lance Lobban, Chair

_____
Dr. Richard Mallinson

_____
Dr. Steven Crossley

Acknowledgements

I would like to thank my girlfriend, Tarah, and my family for all their support during my time at The University of Oklahoma. I would also like to thank the bio-fuels group at OU for the advice and assistance given during my time spent here. I would especially like to thank Dr. Lance Lobban and Dr. Richard Mallinson for all of their guidance during my graduate career.

Table of Contents

List of Tables

List of Figures

Abstract

Industrialization and its long-term effects on the environment are receiving increased scrutiny from both political and environmental pundits questioning environmental sustainability in a time of globalization. Traditional fossil fuels have been the center of criticism for rising carbon emission levels in the Earth's biosphere. A cleaner, renewable, and carbon neutral fuel will be necessary to compete with fossil fuels on the global market if industrialized societies continue to implement policies curtailing emissions. Lignocellulosic biofuels can help fill this role for the planet's energy demands, specifically, thermochemical conversion of lignocellulosic biomass to produce usable hydrocarbon fuels and chemicals. Fast pyrolysis and torrefaction are two methods being developed to produce bio-oil from lignocellulosic biomass. The complexity of the bio-oil mixtures produced from these methods presents technical challenges in the catalytic upgrading of the bio-oil into biofuels and processing of the bio-oil in current industrial equipment. If cost efficient catalysts and process equipment are to be used in the upgrading processes, separation strategies will need to be implemented to simplify and stabilize the bio-oil mixture.

Strategies were studied for the separation of bio-oil vapors from pyrolysis and torrefaction processes through trapping and thermal techniques. Activated carbon acted as the experimental trapping component. Model compounds were used to represent specific compound groups of bio-oil vapors. The effectiveness of these separation strategies was studied using an SRI gas chromatograph through the use of retention times and dynamic temperature profiles employed on the adsorbent trap. Adsorption behavior of the model bio-oil vapor compound groups over activated carbon traps was

also studied with the SRI gas chromatograph and explained as the process in which the adsorbent reaches saturation and excess analyte that does not adsorb travels through the column. The adsorbents were then tested in the use of a pyroprobe to examine separation effectiveness for real bio-oil vapor mixtures. Lastly, the adsorbents of interest were characterized for heats of adsorptions, surface area, pore size, pore volume, and analyte capacity.

Methoxyphenolic compounds in bio-oil vapors adsorb the most strongly to the activated carbon active sites compared to other components found in bio-oil vapors. This strongly bonding principle for methoxyphenolic compounds has been demonstrated by the study of residence time of methoxyphenolic compounds over activated carbon and activated carbon traps implemented in pyrolysis systems. The methoxyphenolic compounds adsorbing stronger than other bio-oil componen is the most desirable outcome for separation of the bio-oil component families as the methoxyphenolic compounds present significant hazards to downstream catalytic upgrading.

It has been observed that levoglucosan in pyrolysis vapors can be thermally trapped onto activated carbon in pyrolysis units.

The capacity and surface characteristics of new and used adsorbents have been analyzed with thermogravimetric analysis and physical adsorption characterization. The capacity analysis has shown methoxyphenolic compounds have the highest capacity of model compounds test at all temperatures. It has been shown that activated carbon loses surface area after use as an adsorbent of model bio-oil compound vapors. This loss in

surface area, however, apparently leads to negligible loss in capacity of the components desired for trapping.

Chapter 1: Literature Review

1.1 Introduction to Biofuels

In recent years there has been a large demand for alternative sources of energy for the growing world's population. This has been fueled by environmental concerns of fossil fuel emissions into the environment, particularly greenhouse gases.[1] Biofuel development and production seeks to provide a sustainable source of energy and fuel for the world; biofuels also produce lower amounts of greenhouse gases than petroleum does. The primary fabrication method of biofuels is transformation from lignocellulosic biomass, such as grasses and woods, to form this sustainable energy and fuel.[2-4] This feedstock of grasses and woods for the production of biofuels has been of more interest in research than other feedstocks as of late, such as fermentation feedstocks like corn, because it does not take away from food sources. One major hurdle that has been hard for this development is difficulty of transforming this biomass into biofuels that can be used effectively by the mass public. The current process for the conversion of this feedstock of lignocellulosic biomass into biofuels is pyrolysis.[3] In the pyrolysis process, the biomass is heated up to high temperatures for a very short period of time; this is typically performed in an inert gas environment, such as nitrogen or helium. When the biomass undergoes this process, it decomposes to a vapor phase of water and smaller oxygenates, including acids, ketones, esters, alcohols, and aldehydes. This mixture is referred to as bio-oil. Bio-oil is extremely unstable because components in the bio-oil are severely oxygenated and are a combination of acids, ketones, esters, alcohols, and aldehydes.[2] The oxygenated compounds have tendencies to perform chemical reactions with one another that are not desirable for upgrading. The storage of

this bio-oil mixture becomes troublesome because these components naturally want to perform unwanted polymerization reactions. These characteristics of the bio-oil mixture would also make the employment into industrial grade refining facilities nearly impossible. This is due to the above mentioned compounds producing acidic environments and degrading process equipment over time. [5] This heavily oxygenated bio-oil mixture is the main reason behind a large development for catalytic upgrading of the bio-oil to firstly deoxygenate this heavily oxygenated mixture. Catalysts used in downstream refining are also of focus for further upgrading into different fuel classes.[2] Deoxygenation is the major focus of the catalytic upgrading process because if pre-existing technologies are to be used for the production of biofuels, the oxygenated compounds have to be addressed before implementation into industrial grade refining facilities.[2] Deoxygenation also has the added benefits of increased carbon yields and improves the properties of the refined bio-fuel.

1.2 Catalytic Deactivation in Vapor Phase Upgrading

Catalytic deactivation is a significant hurdle in refining bio-oil into biofuels to become a sustainable energy source. Catalytic deactivation has been observed to occur very rapidly for various catalysts in certain reactions of interest such as deoxygenation.[6] Catalyst deactivation would occur for the deoxygenation step because of the catalyst's nature in the presence of unstable bio-oil components. Acids and aromatic methoxy compounds in this step produce varying hydrocarbon and poly-aromatic compounds. These compounds produce coke and char which block catalytic active sites. Research at The University of Oklahoma has been ongoing to determine methods to eliminate catalyst deactivation during the deoxygenation step by use of

varying techniques.[7, 8] Few solutions exist that eliminate deactivation through catalysis design. An alternative would be to treat or alter the raw mixture of bio-oil vapors. The mixture contains unstable compounds and the catalyst used to make it more stable cannot endure the barrage of all these compounds at once.[3]

1.3 Fractionation of Bio-oil Components

Separation of the bio-oil vapor mixture could help extend catalyst life and upgrade the mixture more effectively; fractionation was introduced to do exactly this task. Fractionation is used as a method to separate and simplify this mixture but not in the sense of traditional fractionation such as distillation. If traditional distillation is used in this separation process the non-stability of the bio-oil mixture would become very pronounced and the bio-oil vapor mixture would become unworkable. Fractionation is used in the sense that traditionally pyrolysis, as mentioned above, is a one-step process that occurs in a very short period of time and goes to a maximum temperature desired. The fractionation steps being utilized would be a sequence of thermal energy steps with each step in putting more thermal energy into the biomass. The steps of thermal fractionation is referred to as a process known as staged torrefaction. This torrefaction method is theorized to take the raw lignocellulosic biomass components and put them into fractions of the overall bio-oil vapor mixture. The fractions in torrefaction would occur because of an increase in thermochemical stability of varying compound groups in the mixture.[5, 9] The components of the raw biomass that would be fractionated or separated are hemicellulose, cellulose, and lignin. The research currently being performed with collaborators at The University of Oklahoma has used the torrefaction process with these three fractionated stages of thermal treatment and extensive study

has been developed for the upgrading of components in each of these three stages.[10] Different catalysts have been analyzed to upgrade each of the three stages.[7] Pyrolysis of hemicelluloses is the first stage of torrefaction. The thermal conditions for this stage are 270°C for 20 minutes. The products of this stage primarily consist of light oxygenates and water.[9] The second stage of thermal treatment of the biomass solid recovered from the first stage should yield levoglucosan, which derive from the cellulose component.[11] The third and highest thermal treatment of the biomass solid recovered after the second stage of thermal treatment should yield methoxyphenolic compounds, derived from the lignin component.[11] It should be noted that due to the sugar content throughout the biomass, furanics are seen in all three stages of the process because furnanics are a product of sugar pyrolysis.[11] Other compounds from lignin decomposition are scattered throughout the three stages. For the focus of this research, methoxyphenolics, furfural, acetic acid, pyran, and levoglucosan are the compounds of interest.[2, 7, 9, 11]

The main focus of this research will be to selectively trap or separate components for the first stage of torrefaction. The reason the study will be primarily focused on this stage is because the complexity of this stage presents challenges in catalyst design. In Figure 1, Vann shows the product distribution from stage one of torrefaction. It can be observed that the primary components of this stage are acids, esters, and aldehydes. It can also be observed that there are small amounts of phenolic compounds produced as well. The upgrading reaction of interest for this stage is ketonization of the acids, as they are the product produced in largest amounts. The catalyst in which ketonization of these acids occur exhibit deactivation in the presence

of the phenolic compounds. Separation of the phenolic compounds needs to occur to decrease deactivation of catalyst used in ketonization of acids in the first stage. Ketonization of stage one products and phenolic derived deactivation of catalyst will be discussed more in the following sections.

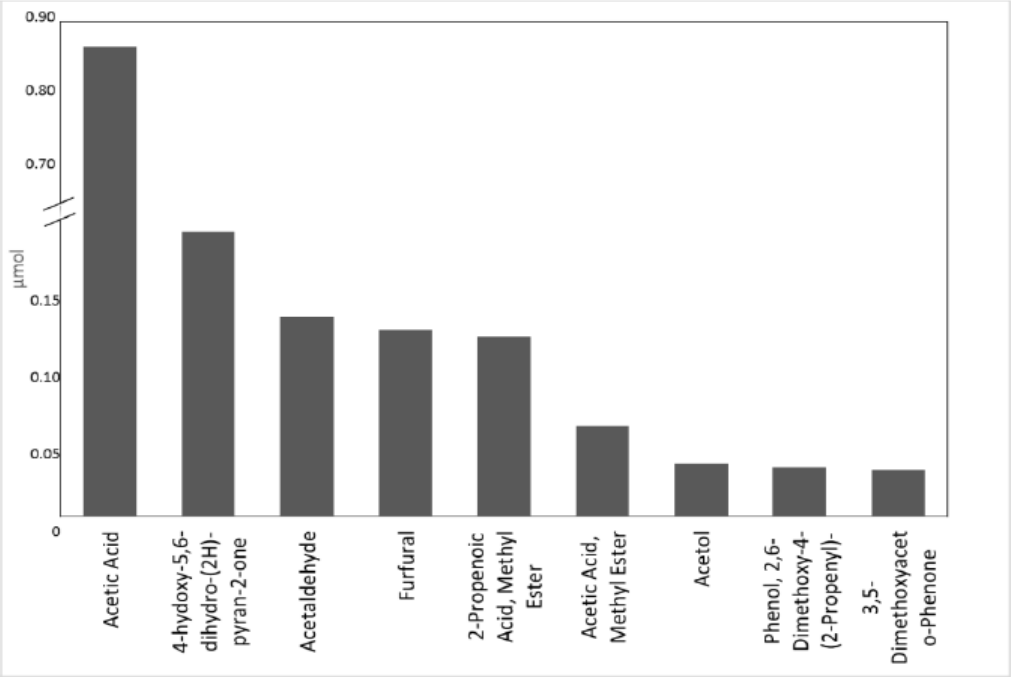

Figure 1: Product distribution from stage 1 torrefaction. Normalized per 1 mg of biomass. Credit Tyler Vann

1.4 Coking of Catalyst during Upgrading Processes

After pyrolysis of these three biomass components, each stream is upgraded separately by the same catalyst or different catalysts, depending on the desired products from the given reactants.[9] Ketonization is desired as the upgrading reaction for the first stage of torrefaction. This reaction would take place on Ru/ TiO_2 as proposed by Pham et al.[7] The ketonization of the stage one products of torrefaction can raise the pH of the bio-oil mixture and decreases oligomerization caused by acids. The ketonization would occur of the acetic acid in the first stage of torrefaction. Two

acetic acid molecules form a carbon-carbon bond with one another while producing a molecule of carbon dioxide. The ketones produced can then be used as building blocks for later reactions to yield higher carbon number compounds, such as aldol condensation.[7] The ketonization also acts as a first stage of deoxygenation for the bio-oil mixture . When any form of deoxygenation takes place on the zeolite, it yields aromatics, hydrocarbons, and coke on the catalyst. This leads to a very quick rate of catalyst deactivation.[12] The amount of coke produced is dependent on several variables, such as the structure and number of active sites the zeolite has, as well as the feedstock and the temperatures used during the torrefaction processes. [12] The reason the coke or char being produced deactivates the catalyst is because they block the active sites on the catalyst where the molecules of interest need to go to be upgraded.[13] Coke is produced inside the catalyst from ongoing reactions. Char is biomass vapors polymerizing on the outside of the catalyst. Coke and char both block reactants from reaching the active sites of the catalyst, causing deactivation.[12, 14] The coke produced inside the catalyst is due to upgraded compounds reacting sequentially with other products and incoming reactants. The sequential side reactions between reactants and products take place until the resulting molecule is too large to exit through the catalysts pores and then continues to react and fill the volume inside the catalyst pore.[12, 14] The main component of the vapor phase that is primarily responsible for the effect of coke formation is aromatic compounds, such as methoxyphenolic compounds and levoglucosan.[15] The coking reaction and process leads to faster catalyst deactivation as shown by Mukarakate et al..[16] The real-time deactivation can be observed for an upgrading reaction in Figure 2 by how the composition of the

product stream is seen changing at varying points in the reaction using gas chromatography:

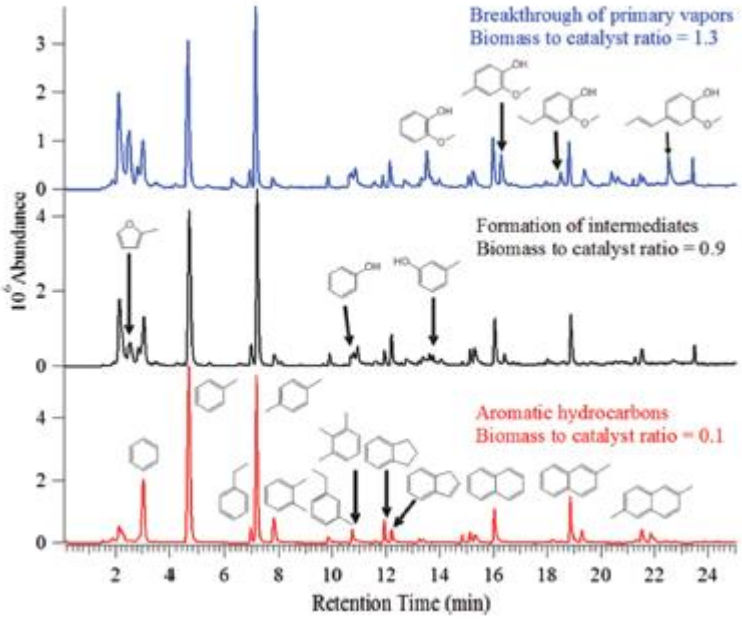

Figure 2:Mukarakate et al. shows 1.0 mg of biomass and 10 mg of HZSM-5 at different points in the experiment.[16]

It is seen in Figure 2 as the reaction progresses, the products move towards poly-aromatic compounds as the biomass to catalyst ratio is decreasing. The product transformation over time is theorized to be contributed to the continual deactivation by ongoing polymerization reactions between reactants and products on the zeolite HZSM-5 active sites in the presence of bio-oil vapors.[16]

1.5 Coke and Char Causing Compounds Analysis and Behavior

The main goal of this research is to selectively adsorb the compounds in the torrefied component stages that cause catalyst deactivation, and to study the way their adsorption occurs. Currently, there is research by Huber et al. and Resasco et al. for catalyst design to decrease the deactivation rate by analyzing how coking is

occurring in the catalyst and how to overcome these processes by altering the zeolite's structure. [9, 10]

The primary contributors for coke formation are aromatic compounds.[17, 18] The targeted aromatic compounds for separation in this research are the levoglucosan and methoxyphenolics that are occurring in the first stage. These compounds occur in the other stages of torrefaction as well, but deactivate the catalyst greatly in the first stage. As recalling for section 1.4, light oxygenates occurring in the first stage of torrefaction are the reactants desired for upgrading. The catalysts over which the light oxygenates are upgraded are highly susceptible for deactivation by the methoxyphenolic compounds and levoglucosan. These compounds have been seen to produce the poly-aromatic compounds that lead to coking of the catalyst and further deactivation by Rezaei et al..[6] In this study, catalyst deactivation was caused by the lignin-derived phenolics. The lignin-derived phenolics occur in the first stage of torrefaction in small enough amounts for feasible trapping. It is theorized by Rezaei et al. that the catalyst deactivation is occurring from the lignin-derived phenolics due to their low reactivity on the zeolites active acidic sites and their prospective probability of strong adsorption on these same sites.[6] It is also shown that the lignin-derived phenolics occupy the zeolite active sites, while not undergoing the desired reaction on these sites. This artifact of methoxyphenolic compounds on zeolites increases the rate of deactivation by blocking active sites.[6] The two catalysts studied were the zeolites, HZSM-5 and HBeta. The larger production of coke due to the lignin-derived phenolics in the catalyst is seen in Table 1. In this table by Rezaei et al., it can be seen that coke is produced in the pyrolysis of cellulose. A lower char and coke yield are occurring in the catalyst due to

the lack of the product of phenolic compounds in this pyrolyzed cellulosic feed. This cellulosic feed primarily produces levoglucosan. This cellulose feed compared to the amount of coke and char produced in the catalyst from upgrading the pyrolyzed lignin feed is much lower. The pyrolysis of the lignin phase of biomass consists of methoxyphenolic compound products. The experiment reaction temperatures are 500°C. Non-catalytic runs are also compared in this table.

Feed	Cellulose	Cellulose	Cellulose	Cellulose	Lignin	Lignin	Lignin	Lignin
Catalyst	Non-catalytic	HBeta	Fe/HBeta	Fe/HBeta	Non-catalytic	HBeta	Fe/HBeta	Fe/HBeta
Carrier gas	N_2	N_2	N_2	H_2	N_2	N_2	N_2	H_2
% Yield								
Oil	30.42	21.38	21.19	20.85	31.30	27.41	24.76	15.90
Gas	33.50	39.16	39.41	39.77	13.24	13.53	14.49	17.83
Aqueous fraction	16.19	18.32	18.52	18.57	9.54	10.83	12.94	18.97
Char/coke	19.89/0	19.71/1.43	19.48/1.40	20.04/0.77	45.92/0	46.10/2.13	45.74/2.07	45.53/1.77

Table 1:Rezaei et al. shows percent yield of phases in fractionation of cellulosic and fractionation of lignin in biomass over zeolite catalyst in inert environments.[6]

Levoglucosan produced in the second stage of torrefaction of the biomass is a cellulosic-derived compound. This stage of thermal treatment in torrefaction is primarily the pyrolysis of the cellulose in biomass.[11] Levoglucosan can increase the rate of deactivation of the upgrading catalyst by means of physisorption onto the surface of the catalyst. This deactivation rate can only occur if the catalyst surface is below the 384°C boiling point of levoglucosan. The torrefaction of the cellulosic component of biomass is at the temperature of 350°C.[11] If the catalyst is held at this temperature, then the chance for physisorption or condensation of the levoglucosan onto the surface of the catalyst is possible. If the levoglucosan becomes condensed onto the surface of the catalyst, sequential reactions can occur with other components of the first or second stage vapors and levoglucosan. These reactions lead to the formation of char on the

catalyst, blocking the catalyst pores and progressing catalyst deactivation. As seen in Table 1, the amount of analyzed char on the catalysts surface is still lower for the cellulosic feed of vapor than for the lignin feed of vapor for both catalysts given.[6] This analysis by Rezaei shows the phenolic products of the lignin feed leads to more char production on the surface of the catalyst than that of the levoglucosan product of the cellulosic feed.[6] For this reason, higher priority will be focused on removing the phenolic products of the first stage of torrefaction. This will ultimately give a larger decrease in the production of char and lower the catalyst deactivation greater than solely removing the levoglucosan from the first stage of torrefaction. Work will be done in this research to remove both but with a larger focus on removing the lignin derived phenolic products.

1.6 Separation Techniques through Adsorptive Traps of Activated Carbon

The desire to remove methoxyphenolic compounds from the first stage is the highest priority to help lower catalyst deactivation rates for upgrading in the first stage. Several approaches have been developed to succeed at this task.[19] In this research, the testing of activated carbon adsorbent to remove the methoxyphenolic compounds from the first stage of torrefaction will be studied. If effective trapping could be achieved of these compound families, catalyst deactivation will be lowered and more suitable or robust catalysts could then upgrade these reactive and unstable compounds once desorbed off of the adsorption trap.[20] If a pure stream of the phenolic compounds can be isolated from the other products of torrefaction stages, Resasco et al. has developed upgrading of these compounds with more suitable catalyst that would involve hydrodeoxygenation followed by alkylation.[22-24] This method would convert the

phenolic compound groups into less reactive cyclic compounds. The catalyst used to upgrade this isolated stream of phenolics is more suitable than the initial catalyst used for the deoxygenation of the stream of products. The catalyst used for the phenolics is a type of metal catalyst. Metal catalysts have better C-O bond cleavage than the initial acidic-site type zeolite catalyst used. This better C-O bond cleavage is ideal for reacting methoxyphenolics.[7] This metal type catalyst also has a lower chance of deactivation from coking when upgrading of the methoxyphenolic compounds is taking place upon it.[7]

Levoglucosan could also be trapped on this adsorbent by thermal methods of condensing the levoglucosan on the adsorbents surface. Levoglucosan is less volatile than the other products found within its stage, making it ideal for physisorption. The trapped levoglucosan could then be volatilized or washed back off the trap and upgraded to more useful products.

In this research a simple adsorbent bed would lie between the pyrolysis or torrefaction reactor and the catalyst bed. The adsorbent beds would be fitted with sufficient pathways to divert desired reactant streams and undesired adsorbing streams to respective catalyst beds or storage units. The easiest way these pathways would be achieved is by an at least 3-way valve. This valve could be switched to a different pathway after a prolonged period of time after elution of the weakly adsorbing compounds took place. This action would divert any trapped compound from reaching a catalyst bed not designed for it. For larger applications, a moving-bed or constant regeneration of adsorbent could be implemented once capacity of the desired adsorbing species was known on a given adsorbent.

Activated carbon is chosen as the adsorbent of interest because of its availability and known ability to adsorb polar molecules, such as phenolic compounds.[25] Activated carbon might also be generated by the pyrolysis and torrefaction processes by taking the biochar that is left from the end of both these two processes and drying, then activating the residual solids with an acidic activation process.[26] This would make the adsorbent readily available in future larger scale applications and simply a by-product of the entire process.

1.7 Phenolic Adsorption on Activated Carbon

Phenolic compounds have been shown by Dabroski et al. to strongly adsorb onto activated carbons.[27] Phenolic compounds are relatively polar compounds and activated carbons surfaces are quite polar as well. The theory we would like to learn from this is why do phenolics adsorb strongly to activated carbon or how do phenolics adsorb strongly. Dabroski's et al. data would give us a deeper understanding of the relationship between these phenolics and activated carbon so better design could occur of the adsorbent.

The main issue in trapping and adsorption of phenolics onto activated carbon is there are many different types of phenolics produced in the pyrolysis and torrefaction processes with all slightly different structures. The phenolics' slightly different structures cause a various range of strengths of which they adsorb onto the activated carbon. The strengths of the adsorptions of the varying types of phenolics produced during the pyrolysis and torrefaction processes is important to know because understanding the different strengths would lead to better design of traps. The varying strengths at which the different phenolic compounds adsorb onto the activated carbon

have been studied by Mattson et al.[28] and Shirgaonskir et al.[29] . The work by these two research groups discusses how the structure of the phenolic compounds affects the strength by which they adsorb and the overall nature of how they adsorb onto the activated carbon. Mattson et al. studied the mechanism by which the phenolic compounds adsorbed onto the activated carbon. What he observed was a hysteresis during the adsorption of phenolic compounds onto activated carbon.[28] The hysteresis is attributed to the reversible adsorption of the phenolic compounds on activated carbon's active sites.[28] Mattson et al. also theorized that the adsorption of the phenolic compounds onto activated carbon followed a donor-acceptor mechanism involving the carboxyl groups on the surface of the activated carbon, with the carboxyl groups being the electron donor and the aromatic ring of the phenolic compounds being the electron acceptor.[28] Mattson demonstrated these phenomena using infrared spectroscopy, by comparing the spectra of pure p-nitrophenol and p-nitrophenol adsorbed onto activated carbon. This is detailed in Figure 3.

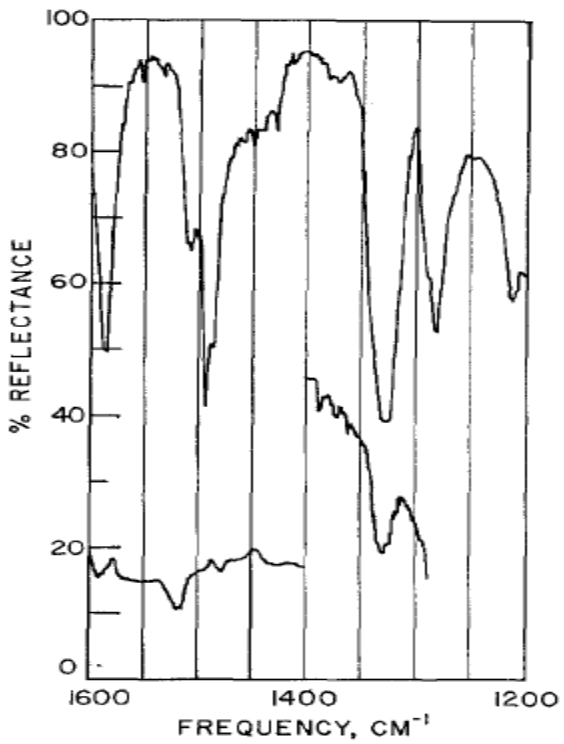

Figure 3:Mattson et al. shows IR-spectrum; The top band being pure p-nitrophenol and the lower bands being the observed bands once adsorbed onto activated carbon

The lower right spectrum in Figure 3 shows that the phenolic C-O vibration adsorbed is in the same position and same shape as the pure p-nitrophenol spectrum above it. The lower left spectrum shows the nitro group peaks are unchanged with respect to the position after adsorption. It is important to note on the spectra the scale expansions on both lower spectra. Importantly, Figure 3 denotes the O-H band has disappeared. The disappearance of the O-H vibration band once adsorbed onto activated carbon is also shown by Mattson et al. in Figure 4.[28] We know from Figure 3 through the previous analysis that the C-O bond remains unchanged after adsorption. This unchanged bond implies that the oxygen cannot be directly associated with the surface, as any interaction occurring would alter the 1330 cm^{-1} in Figure 3.[28] In Figure 4, it is

evident that the phenolic hydrogen is not in an energetically symmetric environment, which reduces the infrared activity by use of atom symmetry.[28] The baseline infrared spectrum for the activated carbon used, KRS-5 is also displayed in Figure 4 to exclude the clean activated carbon from Mattson's analysis.

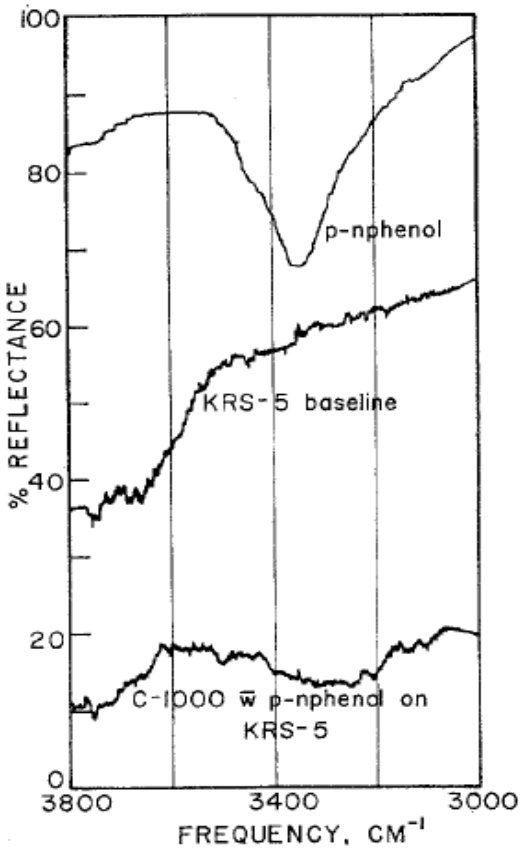

Figure 4:Mattson et al. shows IR-spectrum of O-H vibration period band; The top shows the O-H band of pure p-nitrophenol and the bottom shows the O-H band once adsorbed onto activated carbon

The loss of the phenolic hydrogen does not agree with what is observed with the C-O bond vibration in Figure 3. An atom loss would cause the p-nitrophenol to revert to the most stable quinoid structure of its orientation. This would cause the C-O bond vibration to shift to 1600-1660 cm^{-1} in Figure 2, and is not observed.[28] Additional evidence disclaiming phenolic hydrogen loss is the lack of no observed carbon double

bonds in Figure 3 to the oxygen of the phenolic group, which would form in the absence of the phenolic hydrogen. Mattson et al. attributes this loss to the phenolic hydrogen bonding with the surface of the activated carbon through hydrogen bonding. The contact of the phenolic's aromatic ring with activated carbon is important for this adsorption and greatly influences how strongly the phenolic adsorbs to the activated carbon. Mattson et al. suspects that the phenolic aromatic ring is drawn to the activated carbon because of its pi electron structure.[28] Two factors will greatly influence the strength of the adsorption between the aromatic ring of the phenolic compound and the activated carbon's surface. Electron density of the donor (carboxyl group) and the electron affinity of the acceptor (aromatic ring).[28] The conclusions of the adsorptions of phenolics onto activated carbon is the phenolic C-O vibration is still present after adsorption, the nitro group vibration is still present after adsorption, and the O-H vibration is not present after adsorption but hydrogen bonding couldn't account for all of the interaction of the adsorption. By means of elimination this only leaves the phenolic aromatic ring to interact with the activated carbon and the strength of the interaction is affected by the functional group of the phenolic compound.[28] The polarity of the functional group will determine how well the phenolic aromatic ring will accept the electron from the activated carbons carboxyl groups. The more electronegative the functional group, the stronger the interaction.[28] Mattson determined that the aromatic ring of the phenolic compound was the section of the molecule that the adsorption to activated carbon occurred on by elimination through the IR analysis. By elimination, it is not fully proven that this is the process for adsorption and the phenolic compounds are not simply physisorbing to the activated carbon. The

criteria Mattson described determining the strength of adsorption of the phenolic compound to the activated carbon based upon its functional group structure would also coincide that the heavier molecular weight phenolic compounds would more easily physisorb to the activated carbon. Instead of saying that electronegativity of functional groups determine the strength of the adsorption, another possible explanation is that the more functional groups the phenolic compound has, the heavier the molecule would be, allowing easier physisorption to the activated carbon.

Shirgaonkir et al. tested 24 various phenolic compounds on activated carbon to study the strengths of their adsorptions and what properties affect these strengths. The test was conducted over activated carbon being saturated with phenolic compounds of varying functional groups and the results were analyzed with Freundlich isotherms, determining adsorption constants *k* and *n*. The goal of the experiments was to hypothesize how functional group affects the strength of adsorption on activated carbon. The main conclusions drawn by Shirgaonkir et al.; (1) he number and type of substituent's determine the strength of adsorption, (2) as side chain length increases, adsorption strength increases, (3) the order of strengths of adsorption dependent on functional group of the phenolic compound are as follows, isopropyl>methoxy>methyl>chloro>nitro, and (4) the polarity of the side chain functional group affects the strength of adsorption as more polar functional groups lead to stronger adsorption.[29] Shirgoankir et al. work can be demonstrated in Table 2 by giving the adsorption equilibrium constants, *k.* The conclusions drawn by Shirgaonkir et al. above can be seen to be very similar to the conclusions drawn by Mattson et al.

about the dependence of adsorption strength of phenolic compounds on activated carbon.

compd	Freundlich parameters	
	k	n
phenol	89.43	0.1912
o-chlorophenol	182.1	0.1547
m-chlorophenol	169.1	0.1579
p-chlorophenol	159.1	0.1668
2,3-dichlorophenol	265.2	0.1590
2,4-dichlorophenol	360.2	0.1267
2,5-dichlorophenol	236.16	0.1416
2,6-dichlorophenol	318.02	0.1122
2,4,6-trichlorophenol	588.7	0.1512
o-cresol	255.9	0.1121
m-cresol	167.7	0.1476
p-cresol	181.4	0.1476
2,3-dimethylphenol	217.64	0.1287
2,4-dimethylphenol	253.3	0.1329
2,6-dimethylphenol	326.3	0.1068
3,4-dimethylphenol	283.6	0.1010
3,5-dimethylphenol	218.1	0.1272
o-nitrophenol	147.8	0.3020
p-nitrophenol	166.5	0.1494
o-methoxyphenol	233.14	0.1029
p-methoxyphenol	337.0	0.0777
o-isopropylphenol	320.0	0.0880
p-isopropylphenol	175.8	0.1905
o-hydroxybenzoic acid	86.36	0.2468

Table 2: Shirgoankir et al. shows the dependencies of functional groups on strengths of adsorption of phenolic compounds on activated carbon by adsorption equilibrium constants.[29]

1.8 Literature Conclusions

The theory above shows the applicability of activated carbon to be used as an adsorbent in a trap to remove phenolic compounds from pyrolysis and torrefaction streams. The added benefit of activated carbon is obtaining pure phenolic compounds streams for individual catalytic upgrading. This secures a better carbon balance on the biomass to biofuel process by not wasting these compound groups, and the ability to recover these phenolic compounds from the activated carbon traps. Removal of levoglucosan by thermal trapping from the cellulosic fractionation of torrefaction is also discussed to limit its applicability to coke and deactivate the catalyst. In the next

chapters, the scientific hypothesis of using selective separation and trapping techniques on bio-oil vapor mixtures will be tested.

Chapter 2: Retention Times of Model Bio-oil Vapor Compounds through Gas Chromatography

2.1 Experimental Methodology

2.1.1 Experimental Methodology of SRI-GC

Gas chromatograms were created using a Model 8610C gas chromatograph from SRI Instruments, with nitrogen as the carrier gas. Activated carbon (20-40 mesh, phosphoric acid activated) was the adsorbent used in this adsorption study. The adsorbent was made by Darco and sold by Sigma Aldrich. For the experiment, 0.13 g of the adsorbent was loaded into an eighth inch stainless steel column 10 inches long, and mechanical vibration was used to ensure uniform packing. Each end of the column was plugged with glass wool to prevent loss of adsorbent. All manual injections were performed with a 10µL syringe as the SRI-GC did not have an autosampler.

The solutes employed were acetic acid, m-cresol, 3,4-dihydro-2H-pyran (pyran), furfural, guaiacol, levoglucosan, and syringol. All compounds were injected neat except acetic acid, levoglucosan, and syringol. The acetic acid was injected in the concentration of 2 M in water. The levoglucosan was injected in the concentration of 10% w/w in water, which is 0.6 M in water. The syringol was injected in the concentration of 2.77 M in acetone. The mixtures of the bio-oil vapor components were made by weighing or measuring the volume of the analyte then diluting with solvent using a mechanical pipette to 1 ml. The mechanical pipette's range was 100-1000 µl. The compounds were chosen since they are all commonly found in the torrefaction

stage and pyrolysis processes.[30] The amount of solute injected ranged from 1.0-2.0 μL, and retention time data was collected for each solute at temperatures ranging from 250-375 °C. Retention times were taken as the time it took the compound from injection to first elute off the column to the detector. At least three injections were performed for each solute at the desired temperature to ensure reproducibility. The adsorbent was allowed to regenerate for 12 hours at approximately 300-375°C in 3 psi of nitrogen gas between each injection.

The discharge pressure to the column of the nitrogen carrier gas was set at 3 psi, corresponding to a flowrate of 15 mL/min. The discharge pressures for the hydrogen and air, which were used for the ion detector in the GC system, were set at 20 and 5 psi, corresponding to flowrates of 25 mL/min and 50 mL/min, respectively. All flowrates were measured using an ADM 1000 flowmeter from Agilent Technologies. Retention times of the model bio-oil vapor components were collected over activated carbon at various temperatures to give a first insight of how well the separation may occur of model compounds of bio-oil vapors. The software used to analyze the data from the SRI-GC was Peaksimple provided by SRI instruments.

A depiction of the SRI-GC's flow through the instrument can be seen in Figure 5.

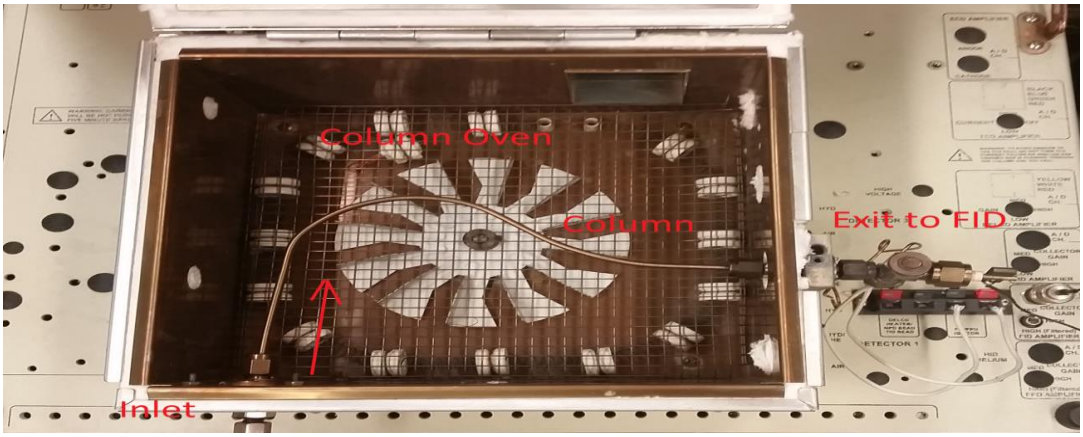

Figure 5: Overhead picture of the SRI Instruments gas chromatographs column and oven.

2.1.2 Experimental Methodology of Pyroprobe

The pyrolysis unit used in the experiments was a CDS Analytical Model 5250T with an autosampler and a cryogenic trap. Pyrolysis vapors travel through heated streams of Silco-Steel transfer lines. The coated stainless steel lines were used to prevent side reactions in the pyrolysis vapors that would normally take place on traditional stainless steel lines. The main heating chamber for the pyroprobe was heated by a platinum coil. This platinum coil could be heated to a specific temperature in a specific time. The flow of inert gas, which was helium, through the pyrolysis unit was 20-90 mL/min. A six-port valve was added to the pyroprobe system to send pyrolysis vapors to a reactor system or directly to a GC-FID/MS system.

The vapors from the pyrolysis system in all cases were sent to a GC-FID/MS system where quantification of the vapors components could occur. A Shimadzu QP2010 system with a RTX-1701 column (60m*0.25mm, 0.25 µm resin thickness) was used. The temperature profile used to separate the components of the bio-oil vapor mixture was 45°C for 4 minutes then a temperature ramp to 280°C at 3°C per minute. The complete program lasted approximately 99 min for each experiment. The split ratio

for the FID/MS detector was 90:1, resulting column flow would be 1 mL/min of inert helium carrier gas.

The FID was used for quantification of the bio-oil vapors components and MS detector was primarily used for identification of the components in the bio-oil vapor. The MS could identify the components through online data bases.[31] The MS could scan masses from 35.00 to 250.00 at a rate of 0.5 seconds per scan. The quantification method used for the FID system was based on the ECN model developed by Nhung Duong at The University of Oklahoma.

The raw biomass being loading into the pyroprobe weighed between 0.7 to 1.0 mg, the weight was dependent on providing adequate peak size in the GC-FID/MS analysis. The raw biomass particle size was 0.25 to 0.45mm and dried under vacuum for 12 hours at 60°C. The composition of the biomass was 21, 47, and 27% lignin, hemicelluloses, and cellulose, respectively. The raw biomass was pyrolyzed at 500°C for these experiments

Two milligrams of activated carbon (20-40 mesh, phosphoric acid activated, Darco) was diluted with 200 milligrams of borosilicate beads. A range of temperatures from 270-330°C was investigated for the trap as pyrolysis vapors flowed over it.

2.2 Results and Discussion

2.2.1 Analysis of Affinity of Adsorbent for Selective Separation of Model Bio-oil Vapor Components

An example of a gas chromatogram of the non-adsorbing gas methane is given in Figure 6 below.

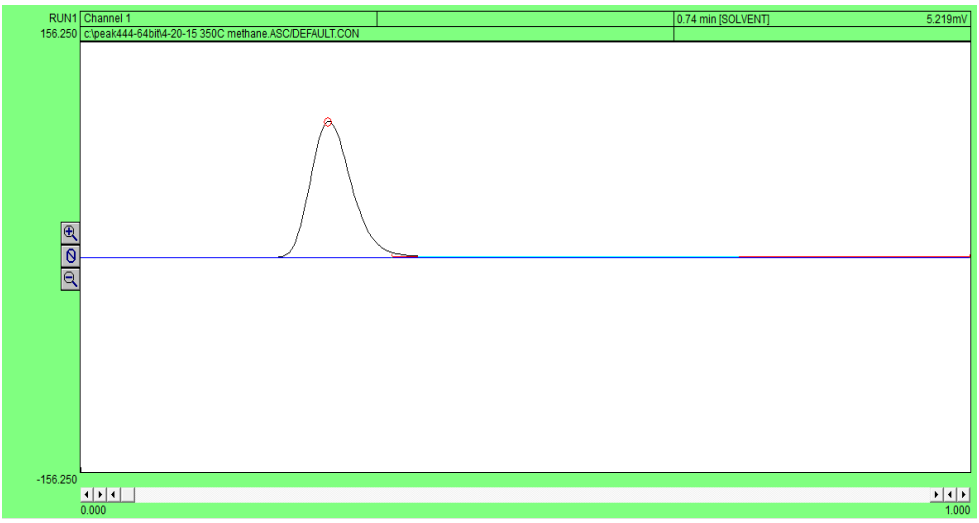

Figure 6: Gas chromatogram of non-adsorbing methane at 350°C

It can be observed from Figure 6 that since methane does not adsorb to the activated carbon, the time it takes it to travel through the column from injection is the time it takes the carrier gas nitrogen to travel through the column. The chromatogram ranges from zero to one minute and has a signal range of +/- 156.25 mV. In this experiment, 1 µl of methane was injected at 0.10 minutes and 350°C. The elution peak begins at 0.22 minutes. The retention time of the methane is then determined to be 0.12 minutes. All other retention times for model bio-oil vapor components were determined in this same manner.

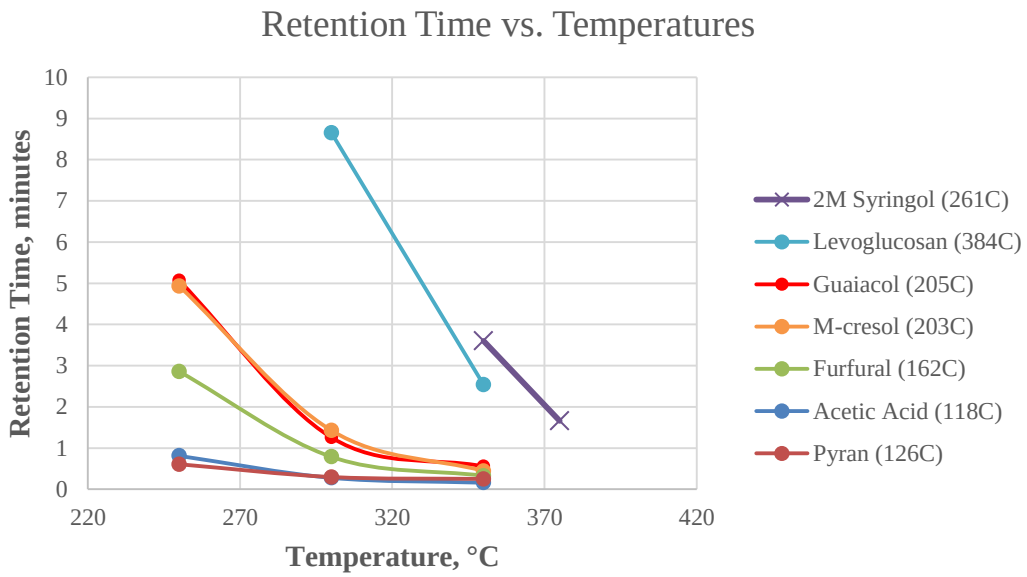

Figure 7: Retention Time vs. Temperature of Various Compounds over Activated Carbon in SRI GC

In Figure 7, the retention times of several compounds at varying temperatures over the activated carbon column are detailed. All injections were 1µL volumes. As seen from Figure 7 at varying temperatures, the components' retention times' increase as temperature are decreased. Figure 7 suggests the capability of the activated carbon trap to separate the model bio-oil components at varying temperatures. The retention time vs. temperature profile for the given components shows for all three temperatures, as the model compounds enter the trap, acetic acid and pyran elute first followed by furfural, guaiacol, m-cresol, and lastly levoglucosan. This separation profile for the activated carbon trap would be beneficial to the downstream refining of bio-oil components because as the phenolic compounds are eluting last, temperature profiles for traps could be designed for refining units which prevent phenolic compounds reaching the catalyst, thereby decreasing catalyst deactivation. The temperature profile

of 250°C was the clearest separation of the components, with the phenolic compounds eluting next to last with levoglucosan. This would be the most promising temperature profile for clean separation of the unwanted components in bio-oil vapor mixtures to ensure downstream refining catalyst life. Regeneration of the traps can occur by increasing the temperature of the adsorbent above 350°C to remove trapped components. This phenomenon is predicted by all retention times given at 350°C between 0 to 3.5 minutes. The larger retention times could be associated with higher bond strengths between the compound and the activated carbon. Another possibility is larger retention times could simply be an artifact of the less volatile components physisorbing to the adsorbent.

Figure 8 includes the standard deviation of the component's retention times for all three temperature profiles. As temperature increased, the retention times decreased. At the lowest temperature profile, the difference in elution times between compound groups is greater than at higher temperature profiles. The lowest temperature profile of 250°C leads to cleaner and more efficient separation of the components than at higher temperatures based on these differences in retention times of the model compounds. In Figure 8 it is important to note that there is no retention time data for levoglucosan at 250°C because of the higher boiling point of levoglucosan. Such trapping would be desirable, for example, to trap levoglucosan from stage one torrefaction products.

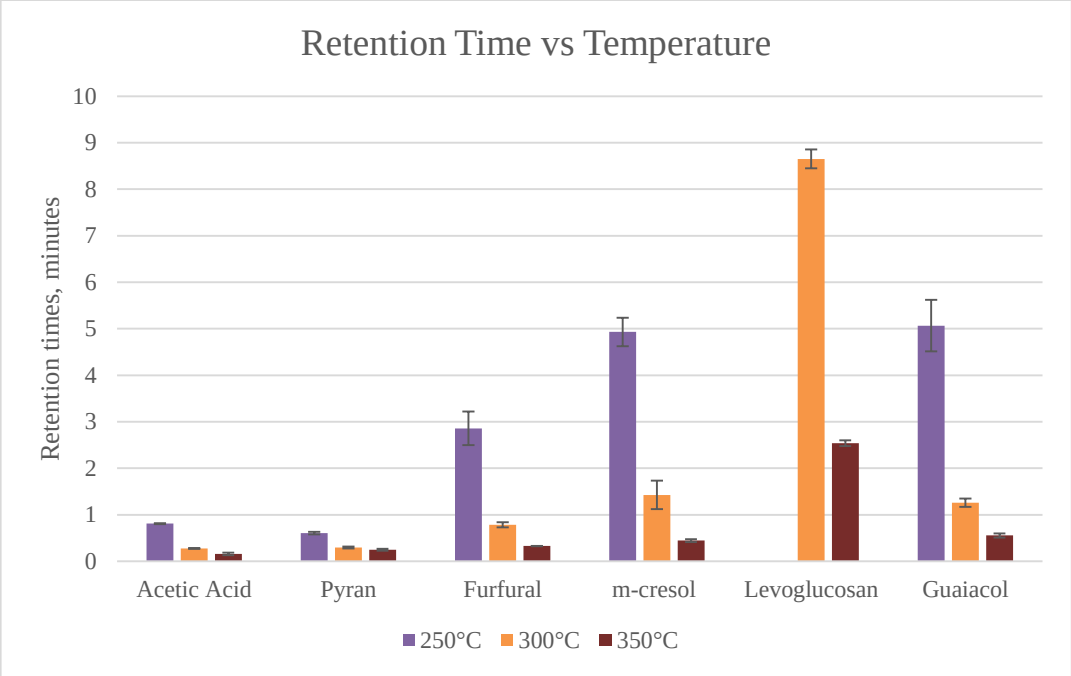

Figure 8: Retention time vs. Temperature for Various Compounds over Activated Carbon with Error

The data shows that it is theoretically possible, with the model compounds of bio-oil chosen, to selectively trap levoglucosan and methoxyphenolic compounds over activated carbon.

The model bio-oil vapor components behaved in alignment with literature observations of adsorption and trap residence time.[28, 29] The phenolics exhibit the longest retention times of any of the model compounds used. This behavior is likely due to their electron donor-acceptor adsorption mechanism. Other model components used and weakly adsorbed have an unknown mechanism of adsorption, such as the pyran, acetic acid, and furfural.

For all standard deviations given in Figure 8, each data point is within the range of approximately 10% of the value of the mean retention time for the vapor compound. The standard deviations found in Figure 8 are calculated from five experiments.

2.2.2 Real Bio-oil Vapor Selective Trapping through Implementation of Trap on Pyrolysis Vapors

A particular component desired to trap is the levoglucosan for stage 2 and 3 of torrefaction. Trapping would be desirable for this compound as upgrading levoglucosan would present less challenges than in vapor phase. As discussed previously, trapping of this component could be achieved by condensation. A high boiling point for levoglucosan (384°C) would allow this possibility.

The model separation of the real bio-oil vapors would exhibit a reduction in levoglucosan and methoxyphenolics. This type of separation mimics the results documented in Chapter 1. Figure 9 provides an insight on how the trapping occurs over activated carbon for real pyrolysis vapors.

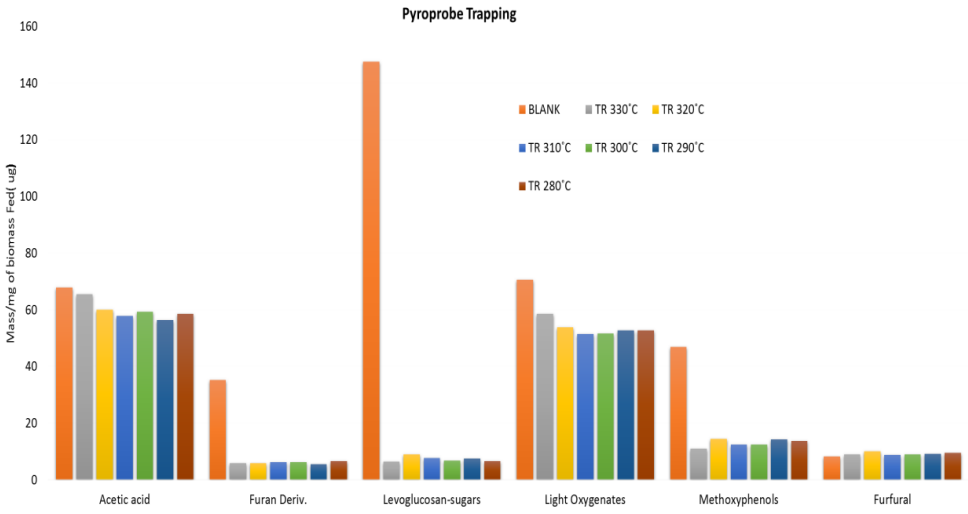

Figure 9: Crossley et al. trapping data at various temperatures taken over an activated carbon bed from vapors of pyrolysis

The graph above plots the trapped mass of products in µg per 1 mg of biomass pyrolyzed at varying temperatures using an activated carbon trap. The components of interest are given on the x-axis. A pyrolysis run without a trap is also given as a blank for comparison. As noted in Chapter 1, strong trapping of the levoglucosan and methoxyphenols is verified from the pyrolysis data at all temperatures at which the activated carbon trap was used. The mixture of components in actual pyrolysis vapors seem to conform to the adsorption data of the single model compounds in the SRI-GC. Only slight trapping of the acetic acid and furfural occur over the trap at any temperature. This behavior is ideal as these components are of interest for downstream upgrading over catalysts and conditions tailored for these compounds, and especially because the levoglucosan and methoxyphenols poison such catalysts. An overall conclusion of the temperature profile shows lower temperatures than the ones given in Figure 9 could be used to gain an even cleaner separation.

Aspects that were not covered by these sets of experiments include recovering trapped material on the activated carbon trap that could be washed off with solvent and recovered in liquid phase or recovered thermally from the trap. These studies were not completed because the pyroprobe sample size was too small, causing difficulties quantifying recovered amounts. In later chapters we will discuss the possibility of further reactions occurring on the surface of the activated carbon.

In the future, the above results would also be desirable to be reproduced over a catalyst bed to determine if trapping these components would lower the rate of catalyst deactivation. The main limitation of this type of study is the FID's sensitivity. It is difficult to quantitatively measure any component that is bleeding off the adsorbent

after more than 1.5 hours of the GC program running. The compounds would not desorb off the activated carbon trap in high enough concentrations for the FID to detect and could be interpreted simply as noise on the chromatograph. Regardless, a diversion valve system would need to be implemented to divert the flow of vapor from the trap after the initial pulse of non-adsorbing bio-oil vapors have passed through the trap to the catalyst bed. The strongly adsorbing species would eventually slowly desorb off the trap and make their way to the catalyst bed deactivating the catalyst if this measure was not put into place.

The error that may be applicable in the pyroprobe component amount data is inefficient measuring of mass of the initial biomass put into the system. This error is still considered negligible as the scientific scales are regularly calibrated.

Chapter 3: Capacity Analysis of Adsorbent for Model Bio-oil Vapor Components through Thermo-Gravimetric Analysis (TGA) and Gas Chromatography

3.1 Experimental and Methodology

3.1.1 Experimental Operation for TGA

The TGA used to measure capacities of model compounds over the adsorbent of interest was a Netzsch STA 449 F1 Jupiter. The TGA can also be coupled with a differential Scanning Calorimeter (DSC), Mass Spectrometer (MS), and Infrared Spectrometer (IR). For our purposes and limitations, only the TGA was utilized to measure the capacity of varying model bio-oil vapor compounds over activated carbon. The furnace type for Netzsch TGA was composed of silicon carbide and had an operating temperature range of ambient to 1600°C, and had a cooling system of forced air. The TGA had a top loading design. The heating rate of the furnace was 0.001 to 50 K/min. The pressure of the furnace could be held at a vacuum of 10^-4 mbar. The instrument comes equipped with 3 mass flow controllers, for 2 purges and 1 protective purge of the sample chamber and loop. The temperature and balance resolution of the instrument was 0.001 K and 0.025 µg, respectively. The maximum sample load of the balance is 5000 mg. The sample volume of the TGA is up to 5 ml.

The activated carbon adsorbent used in the TGA capacity experiments was Darco 20-40 mesh activated carbon (phosphoric acid activated). The surface area of the fresh adsorbent is reported to be 600 m^2/g and has a pore volume of 0.95 cm^3/g. The capacity measurements took approximately 30-50 mg of adsorbent for testing. The adsorbent was pre-treated before the capacity measurement took place to ensure any

moisture and residual compounds were volatilized from the adsorbent's surface and pores. The pre-treatment method was a temperature ramp from 40°C to 300°C at a rate of 5°C/min in the presence of argon flowing past the adsorbent at 20 ml/min, and then held at 300°C and 20ml/min of Argon for 12 hours. The analysis of the adsorbent's capacity is reported at both 100°C and 300°C. The gas flow during the capacity measurements was 40 ml/min of argon and 40 ml/min of air at the 100°C temperature and 80 ml/min of argon at the 300°C temperature. The reason for the varying rates of gas flow over the adsorbent during the two separate temperatures capacities measurement is to eliminate any occurrence of burning the amorphous carbon at the 300°C measurement by removing contact with air. The capacity measurement only took place at these temperatures after the mass of the pre-treated adsorbent had stabilized at these temperatures.

The compounds chosen for testing were of interest because they represented the major compound families that compose bio-oil. The compounds chosen for testing of the 20-40 mesh activated carbon's capacity were syringol, guaiacol, acetic acid, 3,4-dihydro-2H-pyran, and furfural. The syringol and guaiacol were diluted in non-adsorbing acetone for assurance of evaporation in the transfer lines and preventing physisorption onto the activated carbon at 100°C, as the boiling points of syringol and guaiacol are 261°C and 205°C, respectively. The concentrations of the syringol and guaiacol mixtures used were both 2.25 M. The acetic acid used had a concentration of 2 M in acetone to prevent corrosion of non-coated transfer lines, furnace elements, and balance components. All other components used were pulsed in pure concentrations. All component mixtures were made by weighing or measuring volume of analyte and

diluting with a solvent through the use of a mechanical pipette to 1 ml. The mechanical pipette had a range of 100-1000 µl. The analytes were supplied by Sigma Aldrich.

During operation, the analyte was injected in 0.5 µl pulses approximately 30-45 minutes apart through an injection port installed in the purge line of the instrument at ambient temperatures. The flow rates of the purge gases were sufficiently large to volatilize the components at this temperature. After weight gain of the adsorbent was observed to limit or stop with continuing injections, the measurement was concluded. The total weight gain, in mg, was converted to moles of analyte injected and divided by the pre-treated weight of the adsorbent at the beginning of the measurement.

A schematic of the Netzsch STA 449 F1 Jupiter can be seen in Figure 10 below.

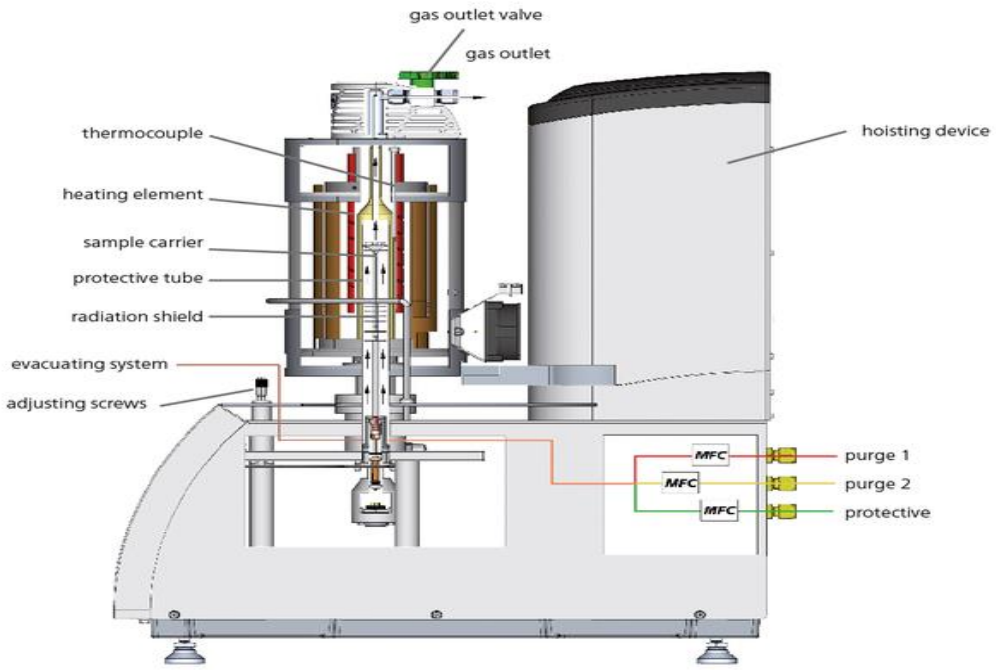

Figure 10: Schematic of the Netzsch STA 449 F1 Jupiter

3.1.2 Experimental Methodology for SRI-GC Capacity Experiments

Gas chromatograms were created using a Model 8610C gas chromatograph from SRI Instruments, with nitrogen as the carrier gas. Activated carbon (100 mesh, phosphoric acid activated) was the adsorbent used in this adsorption study. The adsorbent was made by Darco and sold by Sigma Aldrich. For the experiment, 0.060 g of the adsorbent was loaded into a 1/8 inch OD stainless steel column 2 inches long, and mechanical vibration was used to ensure uniform packing. Each end of the column was plugged with glass wool to prevent loss of adsorbent. The 2 inch stainless steel adsorbent column had to be fitted with 4 inch long, 1/16 inch OD stainless steel tubing with Swagelok adapters so the column had sufficient length to reach from the inlet to the detector of the GC. All manual injections were performed with a 10µL syringe as the SRI-GC did not have an autosampler. A diagram of the SRI-GC and column can be seen in Figure 11 below.

The solutes employed are guaiacol and syringol, in concentrations of 2.78 M in acetone. The compounds were chosen as the model compounds for testing of their capacity on activated carbon because the methoxyphenolic compounds were the only compounds that trapped on the activated carbon long enough for the adsorbent to reach a point of saturation, which is the main principle that needs to occur for a capacity measurement to be observed. Levoglucosan was not tested because at the temperature profiles used, complete physisorption occurs and no elution peak can be detected. All component mixtures were fabricated by weighing or measuring volume and diluting with a solvent through the use of a mechanical pipette. The mechanical pipette had a range of 100-1000 µl. The volume of solute injected ranged from 1.0-8.0 μL, and peak

area was measured for each eluted solute at a temperature of 300 °C. After approximately every 1-3 injections occured injection occurred, regardless of amount injected, the adsorbent was allowed to regenerate at a temperature of 300-375°C for approximately 12 hours.

The general principle of testing the capacity with the SRI-GC is a certain amount of µmol of strongly adsorbing analyte is to be injected over the adsorbent bed. As this amount of analyte changes the elution peak area of the analyte will change as well, by plotting this change in area vs. its respective injection amount of analyte, a trend line can formed depicting roughly when the adsorbent has hit saturation and excess analyte is exiting to the detector. If the adsorbent is not saturated, no analyte elution peak is observed.

The discharge pressure of the nitrogen carrier gas was set at 3 psi, corresponding to a flowrate of 15 mL/min. The discharge pressures for the hydrogen and air, which were used for the ion detector in the GC system, were set at 20 and 5 psi, corresponding to flowrates of 25 mL/min and 50 mL/min, respectively. All flowrates were measured using an ADM 1000 flowmeter from Agilent Technologies. The software used to analyze the data from the SRI-GC was Peaksimple provided by SRI instruments

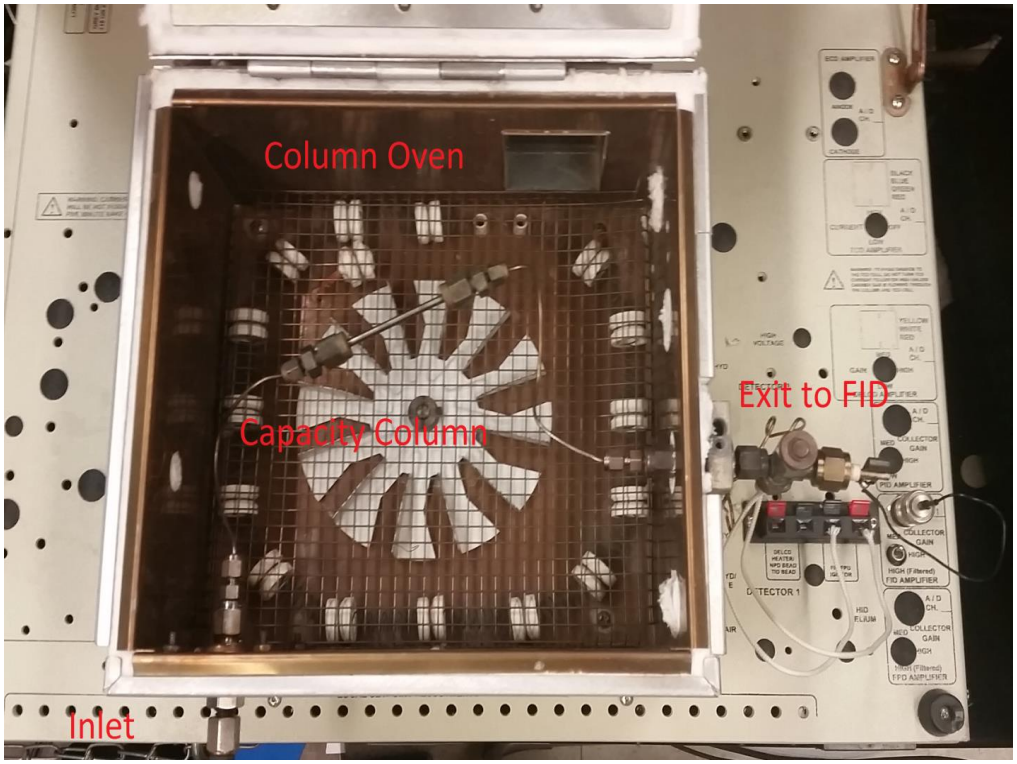

Figure 11: Overhead picture of the SRI Instrument's gas chromatographs column and oven

3.1.3 Experimental and Operational Procedure for Model Bio-oil Component Adsorption over Activated Carbon Using SRI-GC

Column and model compound specifications remain the same as previously given in section of 4.1.2 and the temperature of the column and adsorbent was 300°C. 300°C was chosen because the model bio-oil components will all elute quickly at this temperature and no physisorption is assumed to occur of the less volatile components tested.

In the experimental procedure, 16 µl of 2.78 M syringol were rapidly injected in varying frequencies onto the column of activated carbon adsorbent. Approximately 15 minutes was allowed to pass to observe approximately 44.5 µmol of syringol injected to elute from the column.

3.2 Results and Discussion

3.2.1 Model Bio-oil Component Adsorption over Activated Carbon Using SRI-GC

Work that has been performed previously for studying the adsorption behavior of phenolic compounds, specifically guaiacol, syringol, and cresol, has shown these compounds yield strong adsorption to the surface sites of the activated carbon. The sites on the surface of the activated carbon are carboxylic acid groups.[28] This strength of adsorption of the phenolic compounds onto activated carbon can be recalled by simply accounting for the retention time disparity between these vapor-phase phenolic compounds and other model compounds tested. The phenolic compounds always require longer times to exit a trap than any of the other compounds, besides levoglucosan when the adsorbent is under its boiling point. This length of retention time for the phenolics on activated carbon would suggest stronger adsorption. The adsorptive behavior is in alignment of research performed by Mattson and Shirgoanskir.[28, 29]

The adsorption behavior exhibited by phenolic compounds compared to other model compound groups may be used to trap the phenolic compounds from bio-oil streams prior to feeding to catalytic upgrading reactors.

The strong adsorptive behavior of phenolic compounds is not ideal when trying to measure a quantitative amount of the compound adsorbed to the activated carbon. The challenge this behavior presents is a very slow desorption of the analyte, making integration of FID output peaks very difficult to perform accurately. Quantifying the amount of analyte adsorbed, specifically phenolics, for a given amount of adsorbent is much more suited for Thermogravimetric Analysis, in terms of precision and accuracy

of the measurement, which will be given later in the thesis. The most useful information one can gather from the generated data of the FID, for a strong adsorption in respect to a component of interest, is the process in which the adsorbent becomes saturated by the analyte. The approach to saturation, in respect to the analyte of interest, can be seen in the Figure 12 below.

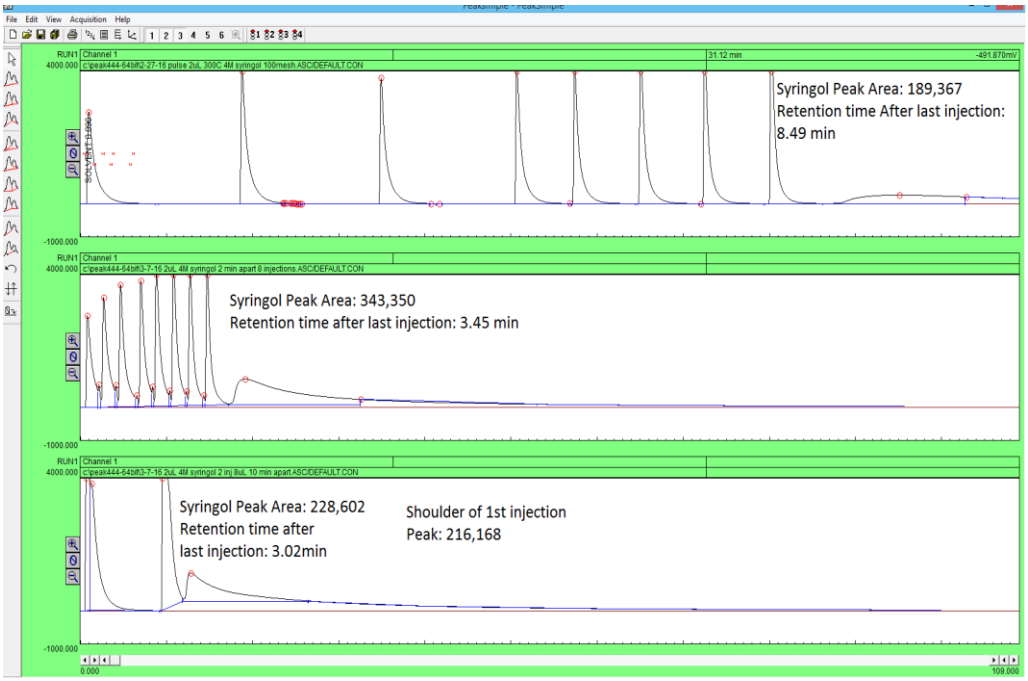

Figure 12: (All injections at 300^{0}C): Top Chromatograph: eight, 2 µl injections of 2.78 molar syringol in acetone done 15 minutes apart for the first four injections then 8 minutes apart for the remaining injections
Middle Chromatograph: eight, 2 µl injections of 2.78 molar syringol in acetone done 2 minutes apart
Bottom Chromatograph: two, 8 µl injections of 2.78 molar syringol in acetone done 10 min apart

In each of the three chromatographs, seen above, the same amount of analyte, or syringol, is injected onto the column. This amount is 44.5 µmoles of syringol. The frequency of the injection and size of sample being injected are the two variables that are changing in these experiments.

It can be theorized that once a given amount of syringol is injected onto the column, the column will become saturated with the analyte and any further injection of the analyte results in any excess amount to pass through the column. Little to no adsorption of the solvent, acetone, is observed, as clear peaks can be seen in each of the chromatographs given.

If the peak eluting last is truly the excess syringol from the last injection that cannot be adsorbed onto the column because the column has reached a point of saturation, then the frequency at which the injections of the analyte take place may have an effect on resolved syringol peaks area due to the adsorbents tendency to slowly desorb over time. The slow desorption of analyte being released from the weaker sites of the adsorbent has a very low concentration so that the FID has difficulty detecting it. Slow desorption of analyte from the adsorbent over time would suggest that as injection frequency decreased, so would the resolved syringol peaks area also decrease. The column still reaches saturation in the top chromatograph but as the column took longer to load with analyte than the trial shown by the middle chromatograph, more time was allowed for a slow desorption of analyte to occur. Consequentially, more vacant sites were present during the last injection of analyte at the point of saturation which resulted in a lower resolved syringol peak area than the resolved syringol peak area in the middle chromatograph.

Injection size near the point of saturation for the adsorbent would also have an effect on the hypothesis of excess syringol moving through the column described above. As injection size decreases near the point of saturation for the adsorbent, the resulting peak from the excess analyte going to the detector will decrease in area as well. Excess

analyte peak area is dependent on size of analyte injected near the point of saturation. Some of the analyte will fully saturate the adsorbent while excess analyte will move through the column and go to the detector. As the injection amount of analyte is increased or decreased, the amount of excess analyte in the column should change correspondingly, and so shall the eluting analyte peaks area change as well.

The adsorption behavior described gives a qualitative understanding of how the adsorbent behaves near saturation. Specifically, how analyte that is not needed for saturation of the adsorbent behaves as it goes through the column. By understanding this adsorption behavior of the column on the SRI-GC, a more accurate experiment can be done to estimate the capacity of the activated carbon using the SRI-GC. These experiments will be performed later in the chapter.

3.2.2 Analysis of Capacities of Model Compounds over Activated Carbon (TGA)

The activated carbon adsorbent was tested for its capacity of the model compounds of real bio-oil vapors. As mentioned previously, the temperatures chosen to test the capacity of the adsorbent were 100°C and 300°C. In Figure 13, a weight gain curve can be seen for activated carbon as furfural is pulsed over it at 100°C.

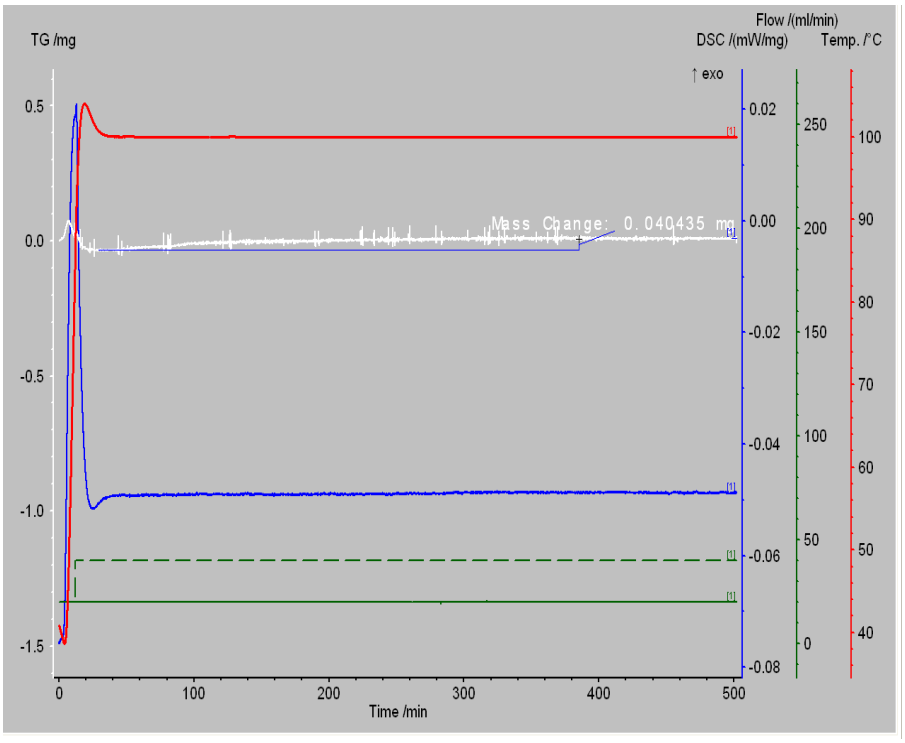

Figure 13: TGA of Furfural over 20-40 mesh activated carbon at 100°C

Detailed in Figure 13 is the weight gain curve of activated carbon as seven, 0.5-µl pulses of furfural were pulsed over the adsorbent. Pulses were performed over the activated carbon until negligible weight gains were observed. It can be observed from the figure the total weight gain of the adsorbent was 0.0404 mg of furfural. The total weight of the adsorbent used was approximately 43 mg of activated carbon. If the amount of furfural gained by the adsorbent is divided by the total weight of the adsorbent then the capacity of furfural on activated carbon is found. Converting to mmols of furfural this value is 0.00963 mmols of furfural per gram of adsorbent at 100°C. All capacities for other model compounds were found with the same method, with the amount of pulses varying to reach a steady mass for the adsorbent

The capacities, in mmol/g, of the adsorbent for these compounds can be seen in Figure 14 below:

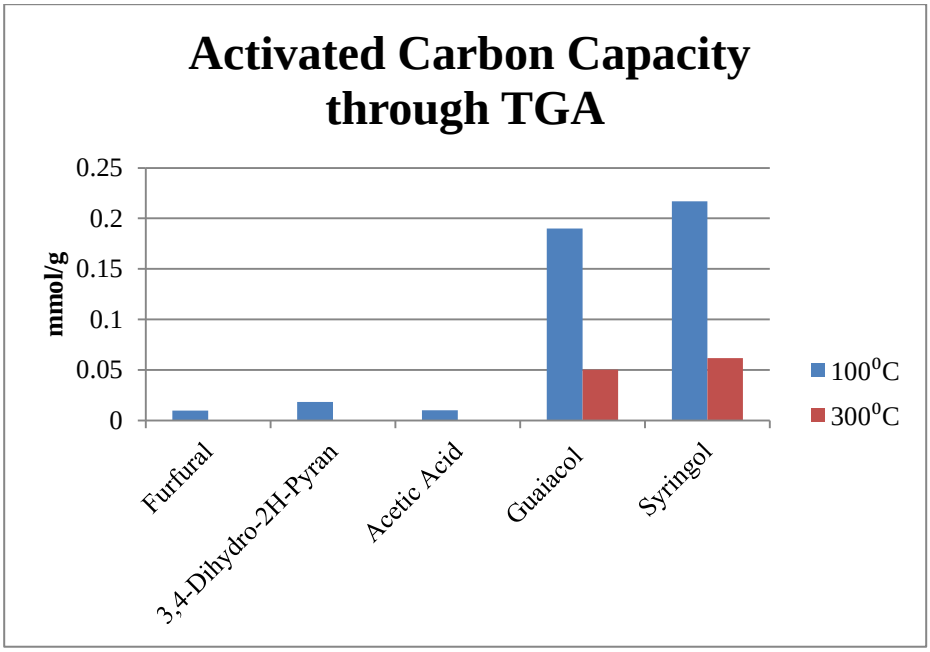

Figure 14: 20-40 mesh activated carbon capacities given by TGA at 100°C and 300°C

It can be easily observed that the methoxyphenolic compounds have larger capacities over the 20-40 mesh activated carbon at both temperatures than any of the other model compounds tested. These larger capacities for the methoxyphenolic compounds would suggest, as mentioned in other chapters, that the phenolic components of bio-oil vapors adsorb more strongly to the activated carbon than other components of the bio-oil vapors. The aldehyde, pyran, and acetic acid model compounds exhibit zero adsorption at 300°C and only minimal affinity for adsorption at the lower temperature of 100°C. The adsorbent temperature of 100°C for actual use of the activated carbon trap over real bio-oil vapors would be difficult to apply because of heavy components found in this mixture physisorbing to the trap, but for the purpose of

finding adsorption affinity of the weaker components tested this temperature needed to be implemented in the TGA study. For the current catalyst design at the University of Oklahoma, these capacity characteristics of the model compounds tested over activated carbon would be ideal for the catalyst used for deoxygenation. Aldehydes, acids, and pyrans of the bio-oil mixtures can all currently be upgraded easily by the catalyst currently being designed for this step, while the methoxyphenolic compounds cannot. As the temperature of the adsorbent is lowered from 300°C to 100°C, it can be observed that the capacity of the methoxyphenolic compounds quadruples over the activated carbon while the other compounds at this temperature range have only a small increase. It is desired for the activated carbon trap to achieve zero to minimal adsorption of the desired components for catalytic upgrading and maximum adsorption of the methoxyphenolic compounds. A precise temperature setting between 100-300°C for the adsorbent would be needed to achieve this goal. The difference in capacities of the components at the varying temperatures would lend guidance to this optimal temperature setting.

We would expect to observe higher capacities for syringol than guaiacol. Syringol has more electron drawing functional groups on the outside of the aromatic ring. This allows for easier acceptance of the electrons from the carboxyl groups on the surface of the activated carbon. If the mechanism of adsorption of phenolics given in chapter 1 theorized by Mattson et al. is correct then syringol would bond more strongly to the activated carbon because of this property. [28] We see this effect for the capacities of syringol and guaiacol given by the TGA, but the difference is negligible as it is only 0.01 mmol/g. Syringol would most likely show stronger adsorption to the

activated carbon because as a heavier molecule, more physisorption would be occurring for the syringol onto activated carbon.

3.2.3 Analysis of Capacities of Model Phenolic Compounds over Activated Carbon (SRI-GC)

The adsorbent's capacity for guaiacol and syringol was also tested in the SRI-GC at 300°C. The experimental parameters can be found above in section 4.1.2. Guaiacol and syringol were the only model components of bio-oil tested with these methods because of their high affinity for adsorption onto the activated carbon traps. The other model components of bio-oil tested, such as aldehydes, acids, and ethers, would pass through the trap and desorb too quickly at this temperature to gain an accurate measurement of capacity. Lower temperatures could have been used in the capacity measurements of the weakly adsorbing model bio-oil components, but quantification of capacity was still difficult through the FID. The quantification of the capacity was difficult because an amount of analyte small enough to be completely trapped could not be performed with the given tools. Even at lower temperatures, the weakly adsorbing model compounds do not adsorb strongly enough to the adsorbent to witness a considerable amount being trapped on the adsorbent with the FID. The adsorptive behavior of the weakly adsorbing bio-oil components can be noted in section 3.2.2 through the use of the more accurate measurement of the TGA.

Figure 15 details two chromatograms at 300°C. Both chromatograms are single injections of 2.78 M syringol in acetone. The top chromatogram has 10.6 µmol of syringol in it and the bottom injection has 15.3 µmol in it. The first peak on both chromatograms is the non-adsorbing solvent, acetone. It can be observed in Figure 15,

that the top chromatogram of 10.6 µmol of syringol shows no secondary elution peak. The secondary elution peak given in the bottom chromatogram of Figure 15 for the 15.3 µmol of syringol is expected to be the eluting syringol. This syringol is the amount of the analyte that was injected and wasn't needed for adsorbent saturation. As excess analyte it then eluted from the column. As the top chromatogram of the injection of 10.6 µmol of syringol has no secondary elution peak, all syringol is assumed trapped on the column.

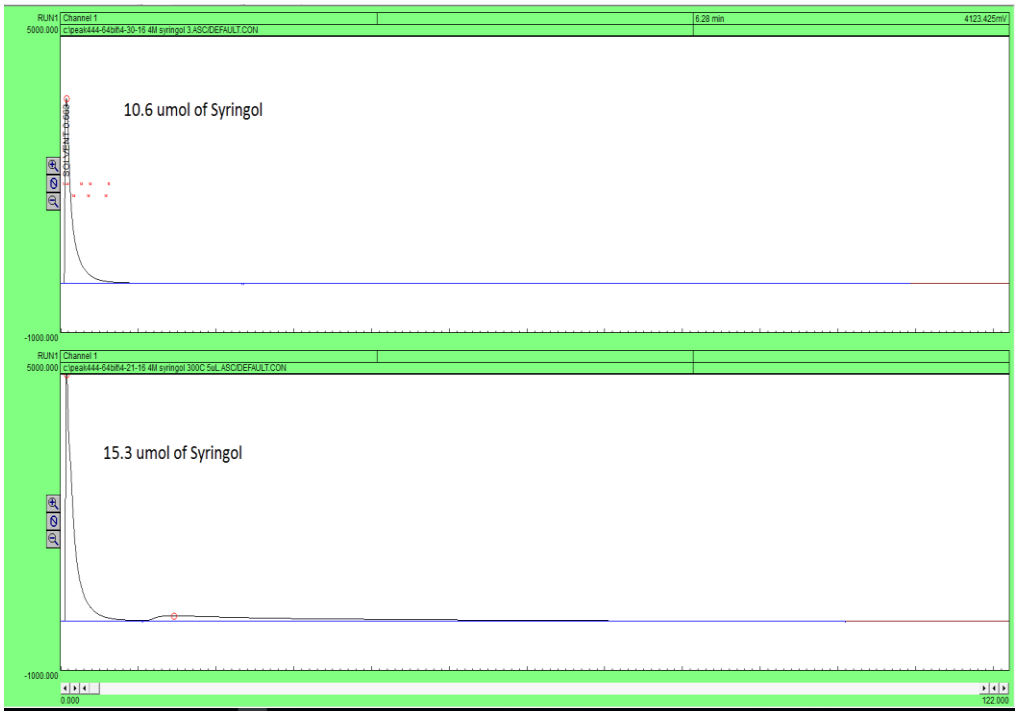

Figure 15: SRI-GC chromatograms at 300^{0}C depicting complete trapping of syringol (top) and excess syringol eluting from column after adsorbent saturation (bottom)

FID peak area given from the eluting analyte peak that is in excess after adsorbent saturation is plotted vs. injection size. This trend from the varying phenolic injection sizes can then be found to find the point at which the analyte first starts to saturate as seen in Figure 16.

Figure 16, below, depicts the FID peak area of the desorbing or excess guaiacol once the saturation of the adsorbent has occurred versus the single injection size of guaiacol onto the column bed of adsorbent.

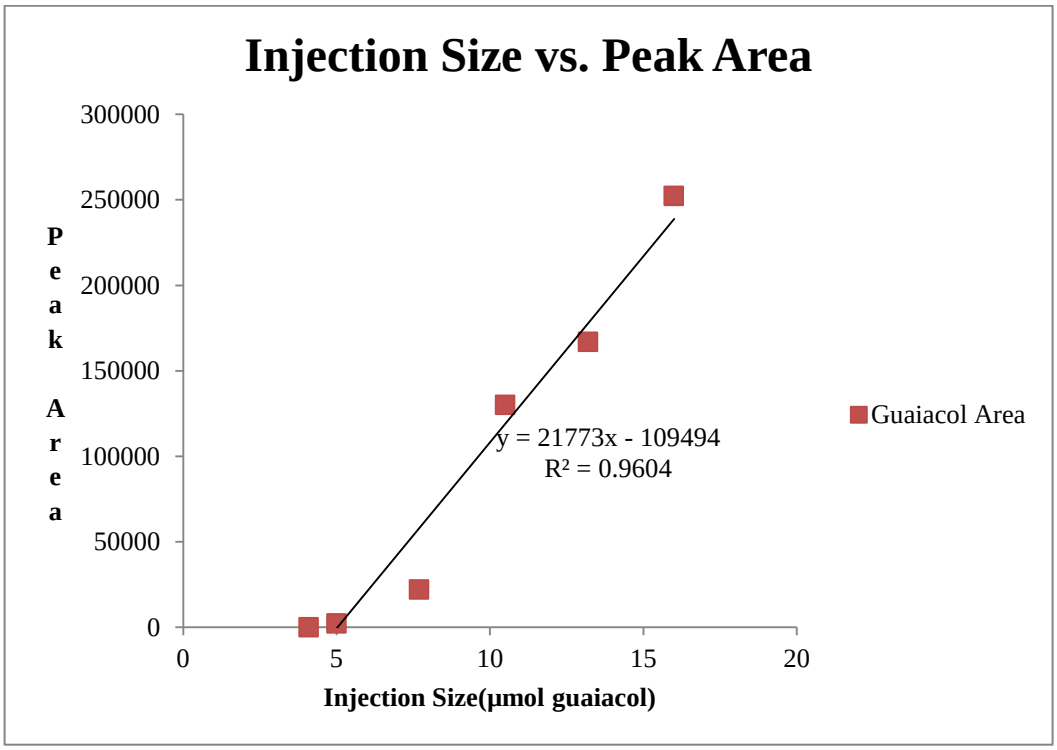

Figure 16: Peak area of eluting guaiacol vs. amount of guaiacol injected over column

At 300°C, the peak area increases linearly with amount of phenolic compound injected. The behavior of the excess eluting phenolic is the same as what is decribed above when the adsorbent becomes saturated and more analyte continues to travel through the adsorbent. It is observed in the injection of just over 4 µmol of guaiacol that the FID peak area is 0, this would be indicative of the activated carbon column trapping all of the analyte injected. When the trend line crosses 0 on the y-axis, the point is taken as when the activated carbon column just reaches saturation of the

analyte. This point for guaiacol is 5.03 µmol. The corresponding capacity for the adsorbent would be 0.0838 mmol/g at 300°C.

Similar methods were used with the SRI-GC for the capacity of the adsorbent for syringol in Figure 17 below:

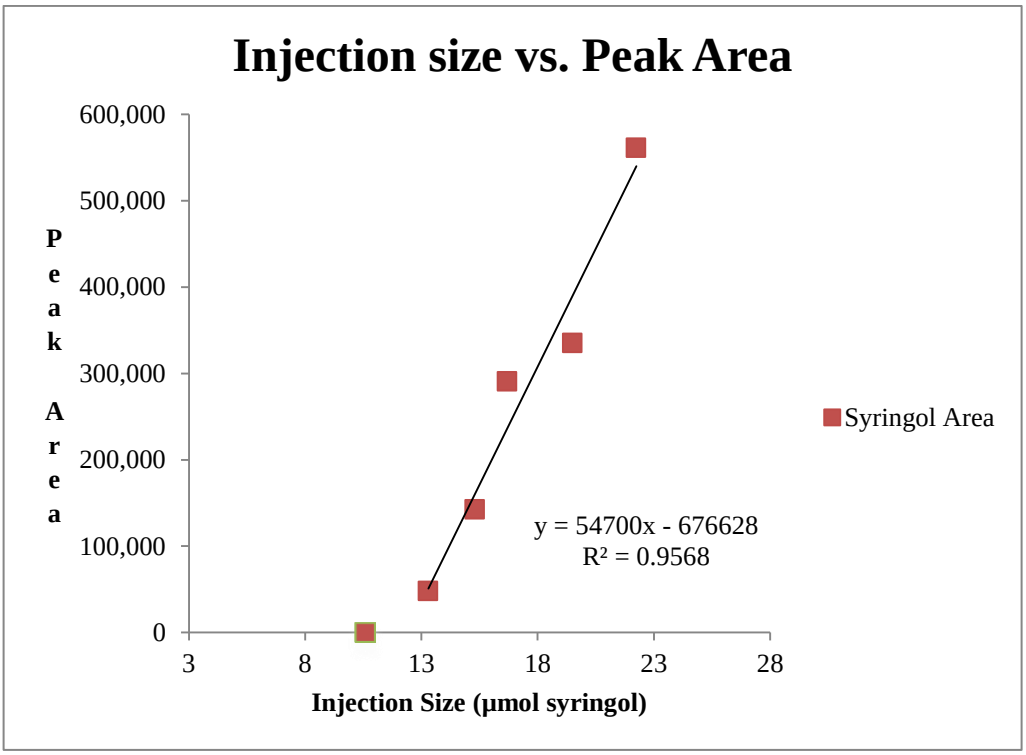

Figure 17: Peak area of eluting syringol vs. amount of syringol injected over column

When the trend line crosses the y-axis at 0 the corresponding saturation of the column is 12.4 µmol of syringol. This gives a capacity of 0.201 mmol/g at 300°C for syringol over the activated carbon.

The capacity measurements at 300°C of the two phenolic measurements tested can be seen in Figure 18 below:

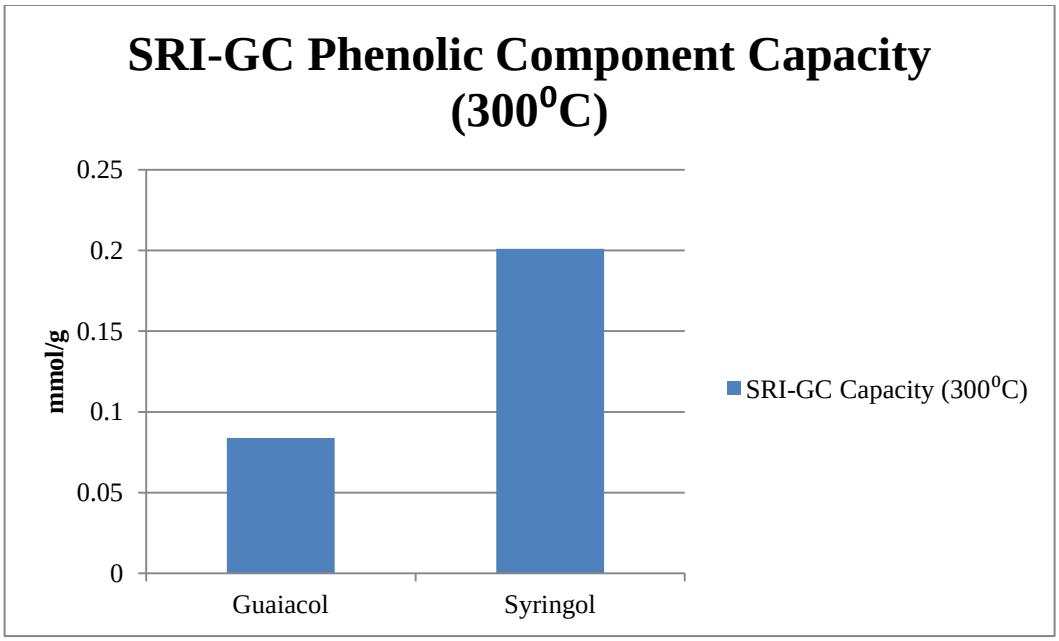

Figure 18: Capacity measurements of guaiacol and syringol over an activated carbon trap

From Figure 18 above, it can be observed that at 300°C the syringol has a higher capacity over the activated carbon than the guaiacol by double. This behavior is indicative of the syringol adsorbing more strongly to the activated carbon than the guaiacol. As mentioned previously, syringol has more electron drawing functional groups on the outside of the aromatic ring, allowing for easier acceptance of the election from the carboxyl groups on the surface of the activated carbon. [28] This characteristic of the mechanism of adsorption of phenolics on activated carbon would not completely explain why syringol has double the capacity of guaiacol at 300°C. If this were true, then we would see similar behavior in the TGA results given above. Another explanation for the difference in adsorption of the phenolics is the syringol is a heavier molecule than the guaiacol, this aspect would allow easier physisorption to the activated

carbon for syringol. This physisorption of the heavier component could be much more pronounced in the SRI-GC than the TGA.

3.3 Summary and Conclusions of Capacity Measurements of Activated Carbon through TGA and SRI-GC

In summary, a comparison of capacity measurements at 300°C given through the TGA and SRI-GC is given in Figure 19 below:

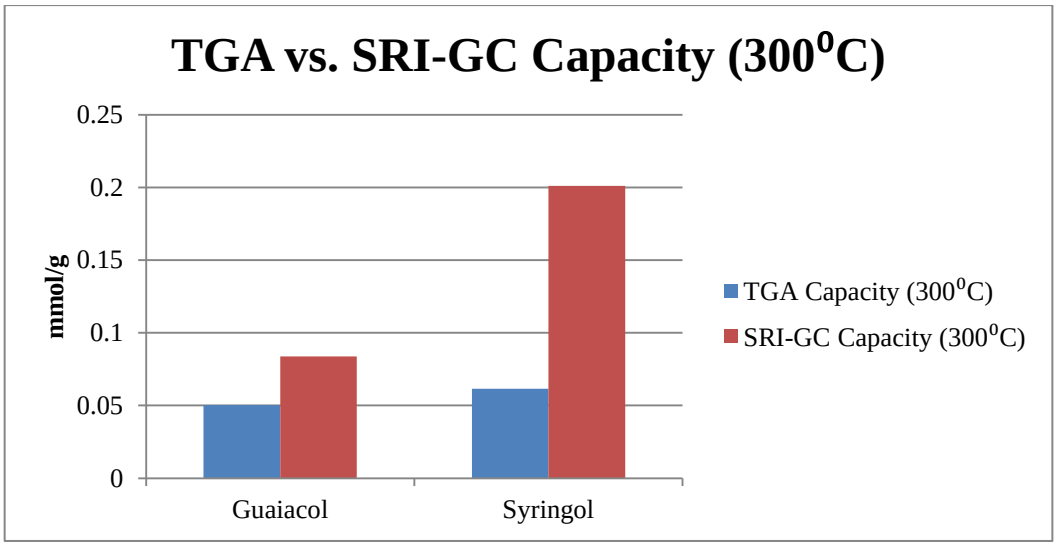

Figure 19: Comparison of the TGA and SRI-GC capacity measurements at 300°C

It is observed from Figure 19 above that the SRI-GC gives larger capacities for both components tested than the TGA at 300°C. The major contribution to this difference is the limitation of detection of the FID. If the analyte is desorbing from the adsorbent very slowly and in small quantities, the FID could not detect it. If the FID did not detect this small amount of analyte eluting, then higher measurements for the saturation point of the adsorbent would be observed. This is because if no peak area of an eluting analyte is observed in the capacity measurements for the SRI-GC, then the adsorbent is assumed to not have reached its saturation point. In reality, the analyte

could slowly be desorbing from the column at this point but in not large enough amounts for the FID to detect, leading to the assumption that everything that is injected onto the column is being trapped. If recalled from the peak area versus injection quantities of the SRI-GC, this phenomenon would make the trend line cross the x-axis at a higher quantity. All injections recorded might have small amounts of analyte desorbing from the column resulting in lost area in the chromatograms. Lost areas in the guaiacol chromatograms due to slow desorption would cause the intercept giving the point of saturation for the adsorbent an artificially high value. This slow rate of desorption may be higher for guaiacol than syringol. This artifact of guaiacol desorption compared to syringol desorption is much more pronounced in the SRI-GC measurements than for TGA measurements due to the sensitivities of the two measurement types. The FID area has more inherent error than the weight gain for the TGA due to limit of detection of the FID compared to the TGA balance.

If implementation of trap is to occur in an actual pyrolysis or torrefaction unit, a diversion valve would be needed to divert the catalyst-fouling phenolics to an alternate catalyst upgrading bed better suited to their chemistries. Timed actuators could achieve this goal, furthering all catalyst lifetimes used in the bio-oil upgrading processes.[6]

The feasibility of the activated carbon trap can be evaluated from the capacities found in the following experiment. The capacity of methoxyphenolic compounds is taken as 0.20 mmols/g at 100°C and the other model compounds capacity on the adsorbent being neglected due to how much lower they are at this temperature. From the pyrolysis group at The University of Oklahoma we assume a pyrolysis of 1000 tons of biomass a day and a liquid yield of this biomass of 25%. The amount of the stage 1

liquid that is methoxyphenolic compounds is 5% on a mass basis. How much activated carbon adsorbent would be needed to completely remove all methoxyphenolic compounds from this stage 1 liquid produced in a day? Appoximately 405 tons of activated carbon would be needed to remove the 12.5 tons of methoxyphenolic compounds from the stage 1 liquid, considering only adsorption of the methoxyphenolic compounds. 405 tons of adsorbent for 1000 tons of biomass is quite a large number but in reality simulated or real moving beds could dramatically lower the amount needed, assuming complete regeneration of adsobent is feasible. Industrial complexes do not use a single bed to selectively separate components over the course of a day. 12.5 tons of methoxyphenolics need to be removed from the process stream daily this means 0.52 tons of methoxyphenolics need to be removed every hour. It would take approximately 17 tons of adsorbent to completely remove 0.52 tons of methoxyphenolic compounds hourly. Two trapping beds would be constructed both of 17 tons of adsorbent. Assuming regeneration of the trapping bed not in use could occur for an hour at elevated temperatures to remove the trapped components. This would decrease the amount of adsorbent needed from one trap of 405 tons to two traps of 34 tons of adsorbent. 34 tons of adsorbent is more feasible on the industrial scale, if all assumptions were held true.

The TGA instrument error should be minimal as the resolution of the balance is 0.025 μg and is regularly calibrated. There would be no other sources of error for the TGA experiments.

Overall, it is evident from the results of both instruments used to test capacity, that the methoxyphenolic compounds have the highest affinity for adsorption for the

activated carbon trap. The results would be in conclusion with the results found in chapter 2. The methoxyphenolic compounds' much higher capacity than the other model compounds on the activated carbon trap validates this theory.

Chapter 4: BET and Capacity Analysis of Fresh and Used Adsorbent

4.1 Experimental and Methodology

The activated carbon adsorbent's surface area, pore volume, and pore diameter were characterized using a Micromeritics ASAP 2020 Plus Instrument. The ASAP 2020 Plus comes equipped with two vacuum systems to allow degassing of two samples and analysis of the primary sample.

The pressure operating range for the instrument is 0 to 950 mmHg with a resolution up to 1*10^-7 torr (0.1 mmHg transducer). The accuracy of the transducer output being more than 0.15% of the reading. The degas manifold can operate from ambient to 450^0C with 1^0C increments. The cooling system has a capacity of 3L for over 72 hours and is a dewar type system. The system also features continuous P_o monitoring. The software used to analyze the results is Microactive for ASAP 2020 Plus.

The method of degassing of the adsorbents was a ramp from ambient temperature to 200^0C by 10^0C/min at a pressure of 10 mmHg, and then held at this temperature and pressure for five hours. The analysis method was a nitrogen isotherm at 77 K with values of quantity adsorbed on the adsorbent being measured as the relative pressure went from zero to one.

The surface area was characterized by the software with the following methods: single point surface area at P/P_o equal to 0.201, BET surface area, Langmuir surface area, 19-point t-plot micropore area, 19-point t-plot external surface area, and BJH adsorption and desorption cumulative surface area of pores. The pore volume was characterized by the software with the following methods: single point adsorption of

total pore volume of pores less than 667 Angstroms at P/P_o equal to 0.970, 19-point t-plot micropore volume, BJH adsorption and desorption cumulative volume of pores. The pore size was characterized by the software with the following methods: adsorption average pore diameter through the BET (4V/A), BJH adsorption and desorption average pore diameter (4V/A), where V is pore volume and A is pore area given either by the BET and BJH characterization methods. A micropore is defined as a pore of 0-20 angstroms in diameter and a mesopore is a pore of 20-500 angstroms. A macropore is defined as a pore larger than 500 angstroms. A more theoretical view of these methods is given by De Lange et al..[32] Since activated carbon has a distribution of pore sizes, a robust analysis method is needed. The analysis needs to gather multiple points of quantity adsorbed as P/P_o goes from 0 to 0.2 so an accurate measurement of the micropores' surface area and volume can occur. The 19-point t-plot achieves this measurement within the range of P/P_o most efficiently. Similarly, multiple points of quantity adsorbed are needed as P/P_o goes from 0.5 to 1 to gain an accurate measurement of the mesopores' and macropores' surface area and volume. The BET and BJH adsorption and desorption methods achieve these measurements the most efficiently for the adsorbent tested. Overall, the BET, BJH, and t-plot methods are the most accurate methods to use in measuring the surface and pore characteristics of activated carbon according to Leofanti et al. [33]

The activated carbons used in the experiment were Darco 20-40 mesh and 100 mesh, both activated by the phosphoric acid process. The specifications of the fresh adsorbents were both 600 m^2/g for the surface area and 0.95 cm^3/g for the pore volume given by Darco. The 20-40 mesh used adsorbent had approximately 800 µL of

analyte injected over the 130 mg being tested and had been regenerated approximately 250 times at 300-375^{0}C for 12 hours each time. The 100 mesh used adsorbent had approximately 225 µL of analyte injected over the 60 mg being tested and had been regenerated approximately 213 times at 300-375^{0}C for 12 hours. The analytes being injected over the used activated carbon were furfural, acetic acid, 3,4-dihydro-2H-pyran, guaiacol, m-cresol, syringol, acetone, and levoglucosan, as these were the model compounds being tested to mimic the main compound families of real bio-oil vapors. All analytes were supplied by Sigma Aldrich.

A picture of the Micromeritics ASAP 2020 Plus can be seen in Figure 20:

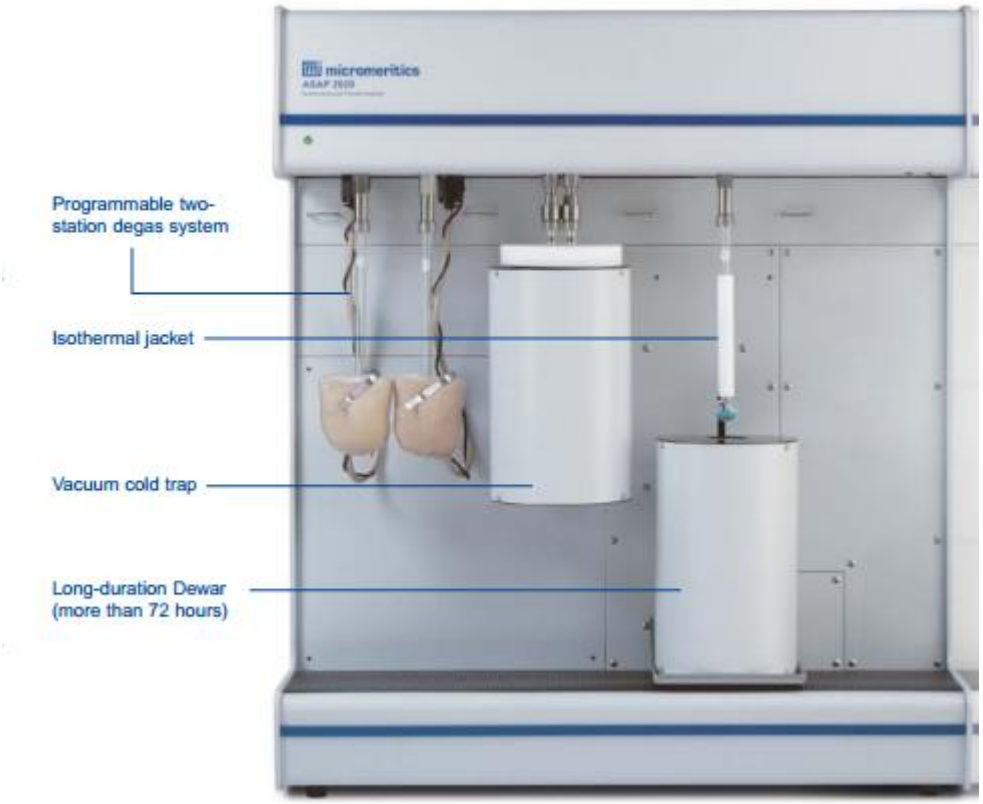

Figure 20: Micromeritics ASAP 2020 Plus Instrument

4.2 Results and Discussion

The following analysis is used to answer if, after selective trapping occurs of the model bio-oil compounds and regeneration takes place on the activated carbon trap, do the surface and pore characteristics of the activated carbon change. If a change in these characteristics is observable, it would imply even after regeneration of the activated carbon trap occurs, irreversible adsorption may be occurring on the activated carbon trap of the analytes injected. Once irreversible adsorption occurs of these analytes on the surface or in the pores of the activated carbon, they may have a tendency to form coke or char on the surface or in the pores of the activated carbon. If coke and char formation is occurring on the activated carbon, then the surface area of the adsorbent would be decreased due to pore mouths being blocked or a pore completely plugging with residual organics being left after trapping takes place. The decrease of total surface area would of course be due to the fact that the surface area the inside of the pores contributes to the total surface area of the adsorbent is now inaccessible. Another interesting observation would be if a decrease in surface area is shown, what sizes of pores are most affected by this? An analysis of pore volume and diameter of fresh and used adsorbent can give insight to this question. The comparisons of the fresh and used adsorbents' pore volume and diameter will also give insight to which size of pores is the trapping of the analytes occurring by showing whether the adsorbent's micropore or mesopore volume is decreasing greater than the other. The pore diameter analysis also contributes to this question by showing if the average pore's diameter is increasing or decreasing between the fresh and used adsorbent. This measurement would indicate if

the smaller or larger pores become the dominant site for analyte adsorption and later plugged or covered with irreversible adsorptive products.

In the first analysis, the surface areas of the 20-40 mesh and 100 mesh are examined by the BET with the varying techniques. It is important to note that some of these surface areas given are total surface areas of pores and external surfaces . The others given are just the surface areas of pores, methods of this case are the BJH method and the t-plot micropore area method. External surfaces are defined by Leofanti et al. as the surface of the catalyst adsorption is taking place once all micropores are filled. [33] External surface areas are only measured once the micropores have reached maximum adsorption.

The surface area analysis of the 20-40 mesh fresh and used activated carbon adsorbent can be seen in Figure 21 below.

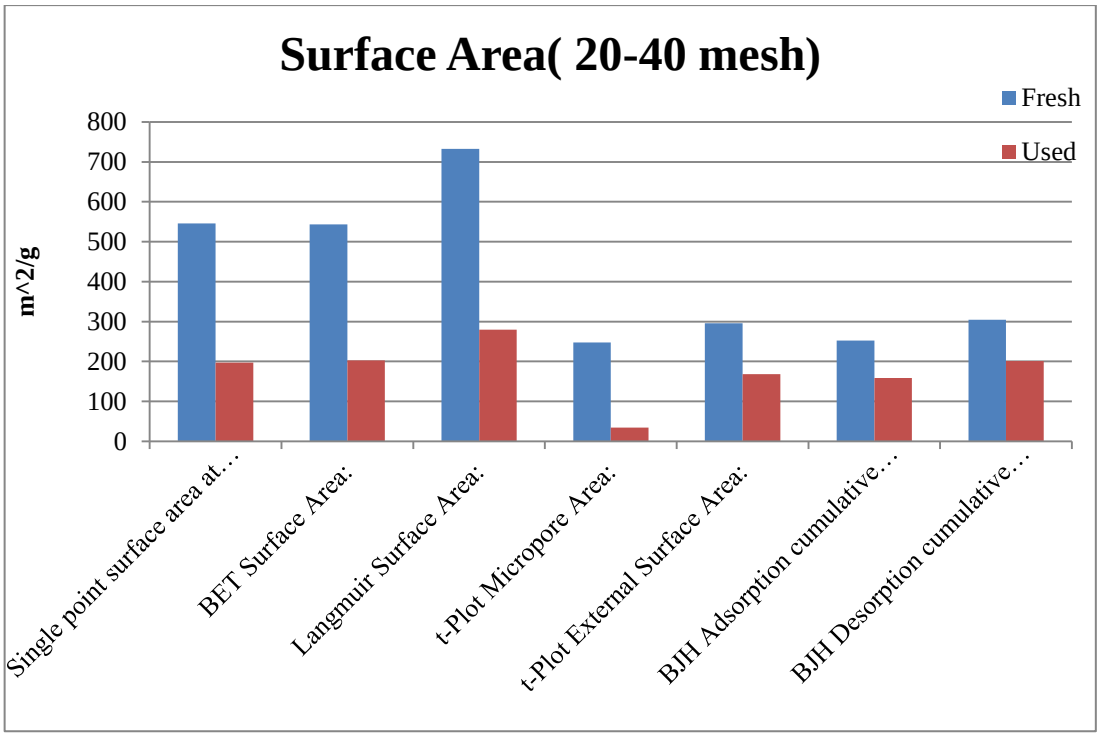

Figure 21: Surface area of fresh and used 20-40 mesh activated carbon

A decrease in surface area is seen between the fresh and used adsorbent in all measures detailed in Figure 21. Of the methods used to analyze the surface area, the single-point, BET, and Langmuir surface areas give the area of the adsorbents' pores and external surfaces added together. The t-plot gives the surface area of the micropores and external surfaces separately. Lastly, the BJH method gives only the area of pores in diameter of 17-3000 angstroms through an adsorption and desorption isotherm. The specifications for the 20-40 and 100 mesh activated carbons is 600 m^2/g for the surface area. While some of the analysis methods are not close to this specification, all activated carbons were analyzed with the same methods for a base comparison of these characteristics. The analysis method that is most intriguing in these experiments is the t-plot micropore and external surface area analysis. The t-plot analyses combined surface areas add the most closely to the specification given by the supplier. The area from the micropores in this method decreases by 86% between new and used adsorbent. The area from the external surface in this method decreases by only 43%. It can be observed that most of the surface area decrease is in the micropores. The BJH adsorption and desorption analysis of the surface area of the pores does not show a dramatic decrease between fresh and used adsorbent as the t-plot analysis. This result might be to contribute to the BJH analysis only measures the surface area of pores with diameters between 17-3000 angstroms. The larger diameter pores might not be decreasing in surface area as much as the micropores, these phenomena will be looked at more extensively in the analysis of the pore volume and diameter changes between the fresh and used adsorbent.

In Figure 22, given below, the surface area through the varying analysis of the 100 mesh fresh and used activated carbon is given.

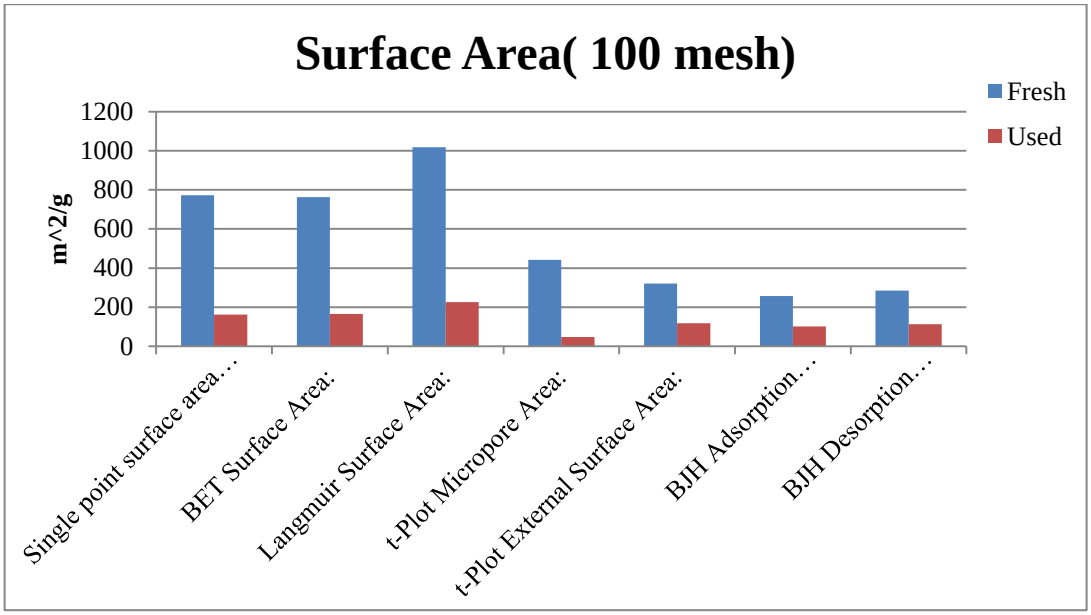

Figure 22: Surface area of fresh and used 100 mesh activated carbon

It can be observed that the 100 mesh activated carbon behaves similarly to the 20-40 mesh activated carbon, in which a clear decrease in surface area between the fresh and used adsorbent can be seen. The micropore surface area given through the t-plot analysis shows a 90% decrease while the external surface area shows a 60% decrease between fresh and used adsorbent. This characteristic of 100 mesh used activated carbon is also very similar to what was observed between the fresh and used 20-40 mesh activated carbon, therefore, similar conclusions can be drawn. Overall, the 100 mesh adsorbent is exhibiting a larger decrease in surface area than the 20-40 mesh. This result might be due to a larger percentage of the analyte injected over the 100 mesh adsorbent being strongly adsorbing phenolic compounds. Phenolic compounds are suspected to be the molecules undergoing irreversible adsorption onto the activated

carbon. Phenolic compounds are assumed to be undergoing this process on activated carbon as they do on zeolite catatlyst, only not to of great as an extent because of weaker adsorption sites. Rezaei et al. first reported this behavior for HZSM-5 and H-beta catalyst in the presence of phenolic compounds.[6] From the capacity studies in chapter 4, it is also observed that no other compounds classes tested besides phenolics adsorb in large quantities at the temperature the used adsorbent was held at during adsorption experiments (300^0C). This only leaves the phenolic compounds to adsorb onto the used activated carbon irreversibly, causing a decrease in surface area of the adsorbent.

To better understand the decrease in the surface areas of the adsorbent, an analysis of the pores volume and diameter is needed. In the analysis of the pores volume, the methods of the analysis were a single point adsorption to determine the pore volume of pores less than 753 angstroms in diameter, a t-plot micropore volume, and BJH adsorption and desorption analysis for volume of pores between 17-3000 angstroms in diameter. The specifications of the pore volume for both the 20-40 mesh and the 100 mesh activated carbons is 0.95 cm^3/g, given by Sigma Aldrich. A pore volume analysis of the 20-40 mesh activated carbon is given in Figure 23 below.

Once again, as in the analysis of surface area, a decrease in pore volume can be observed in the 20-40 mesh adsorbent. It can also be observed from the chart that in the t-plot micropore analysis, the largest decrease in pore volume is occurring of 90% reduction in volume. All the other methods of analysis for the pore volume between the fresh and used adsorbent show a decrease of approximately 25%.

The decrease in volume between the fresh and used adsorbent of the analyses measuring volume of the pores larger than micropores is smaller than the analyses only measuring micropores volumes change.

If the fresh adsorbents volume would be filled completely with methoxyphenolics, then each gram of adsorbent would hold 3.7 mmol of syringol. From the capacity measurements in chapter 4, we know this is not the case. The actual capacity of syringol is 0.2 mmol/g. The syringol being adsorbed onto the activated carbon is only occupying 5% of the adsorbent's pore volume.

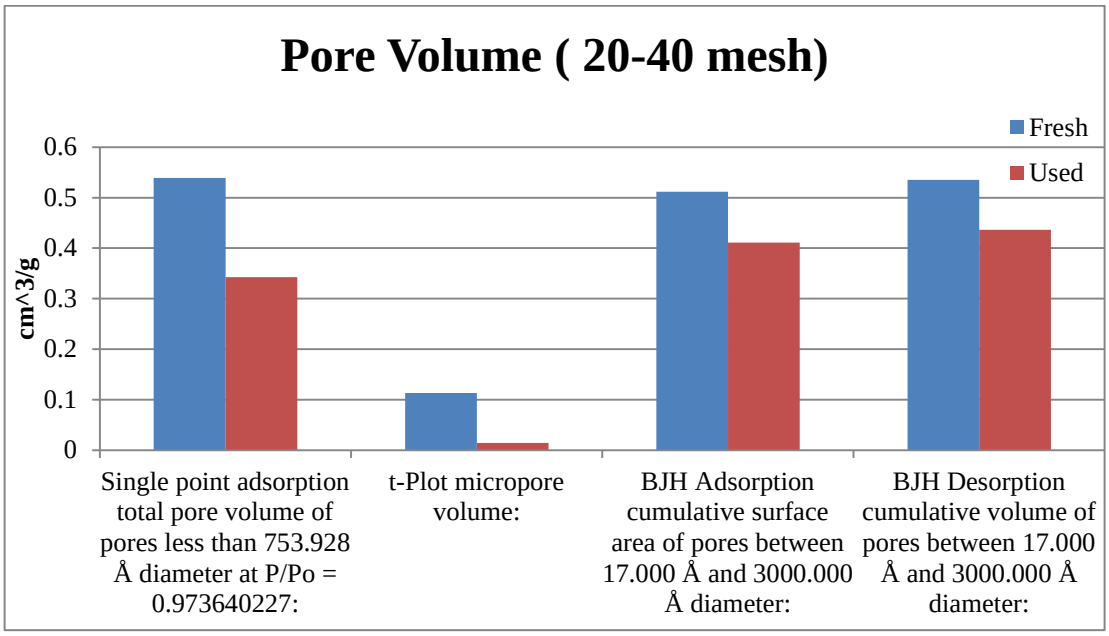

Figure 23: Pore volume of fresh and used 20-40 mesh activated carbon

In Figure 24, given below, the analysis of the pore volume can be seen for the 100 mesh activated carbon. Similar behavior is once again observed for the 100 mesh activated carbon as was seen in the 20-40 mesh activated carbon. A greater decrease is observed in the micropore volume than the mesopores of the adsorbent after use. The decrease in micropore volume between the fresh and used adsorbent for the 100 mesh

particles is 90% . The decrease in all other pores volume between the fresh and used adsorbent for the 100 mesh particles is approximately 50%. As the ratios of the pore volumes for the fresh and used 100 mesh adsorbent are similar to the 20-40 mesh adsorbent, similar conclusions can be drawn from the pore volume analysis. The micropores of the adsorbents in both cases lose more volume compared to the larger pores of the particle. The 100 mesh adsorbent could theoretically hold 3.5 mmol of syringol per gram of adsorbent. The capacity for the 100 mesh adsorbent at 100^0C for syringol is actually 0.2 mmol/g. The syringol being adsorbed onto the activated carbon is only occupying 5% of the 100 mesh adsorbent's pore volume.

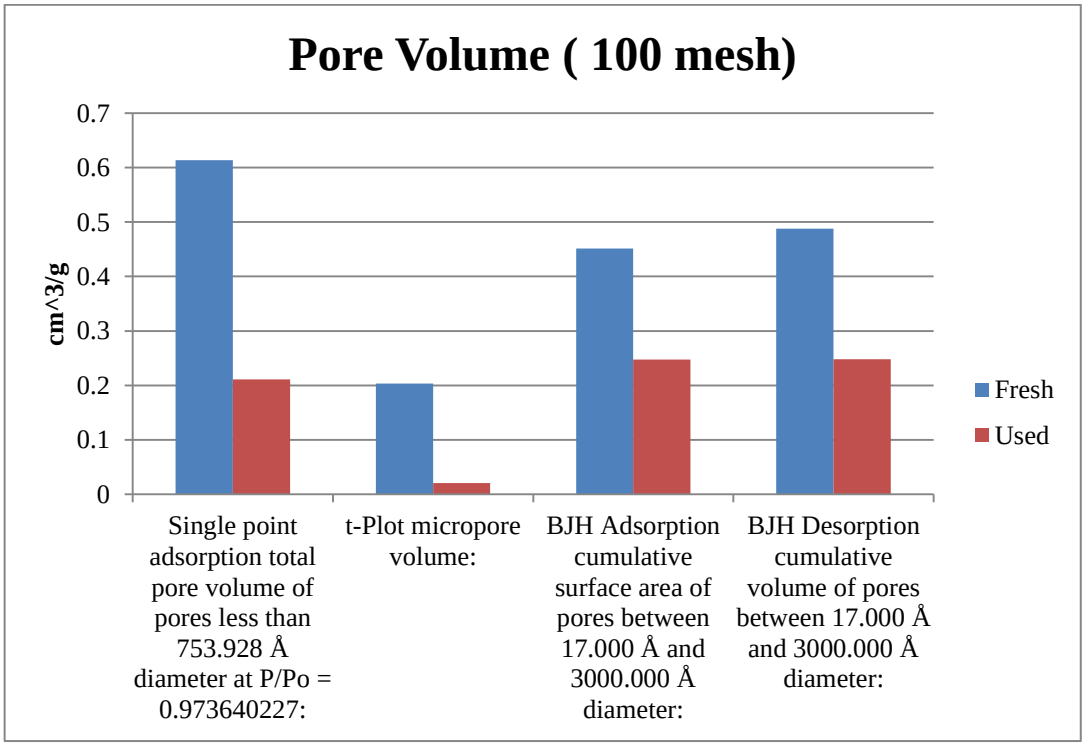

Figure 24: Pore volume of fresh and used 100 mesh activated carbon

An analysis of the fresh and used pore diameter characteristics are examined. If the current trend continues as in the analysis of surface area and pore volume of the adsorbents, we should see an average pore size increasing between the fresh and used adsorbent. As micropore surface area and pore volume is decreasing for fresh to used adsorbent, fewer micropores are assumed to be available in the adsorbent. The lower population of micropores would make the average pore diameter increase.

In Figure 25, given below, an average pore size comparison between the fresh and used adsorbent for both particle sizes is shown.

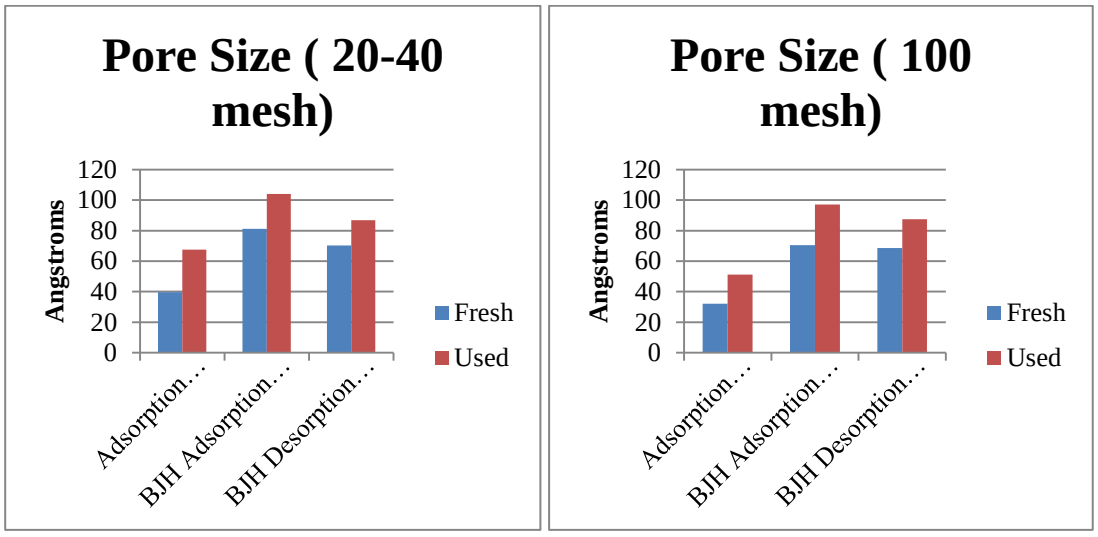

Figure 25: Pore size analysis of fresh and used 20-40 and 100 mesh activated carbon

The behavior predicted above can be observed to take place in Figure 25 for both sizes of particles, in which the average pore diameter is increasing for all analysis methods used. It can also be observed that for both sizes of particles the increase in pore size between the fresh and used adsorbent is approximately 40%.

In Figure 26, the capacity of syringol was tested over 100 mesh fresh and used adsorbent using the SRI-GC method explained in chapter 3. The capacity measurement

between the new and used adsorbent would chronicle if the loss of micropores would affect the efficiency of the adsorbent. Both capacity measurements took place at 300^{0}C. The syringol used for the injection was 2.77 M in acetone. The solution was made by adding 4 mmols of syringol to 1 ml of acetone. Only the syringol capacity was tested over both adsorbents as it has the highest capacity of all compounds tested so any decreases would be easy to observe. The syringol being a methoxyphenolic compound is also the main compound family that is desired to be trapped by the adsorbent in real bio-oil vapors. This makes it of great importance to ensure its capacity stays the same over used adsorbents.

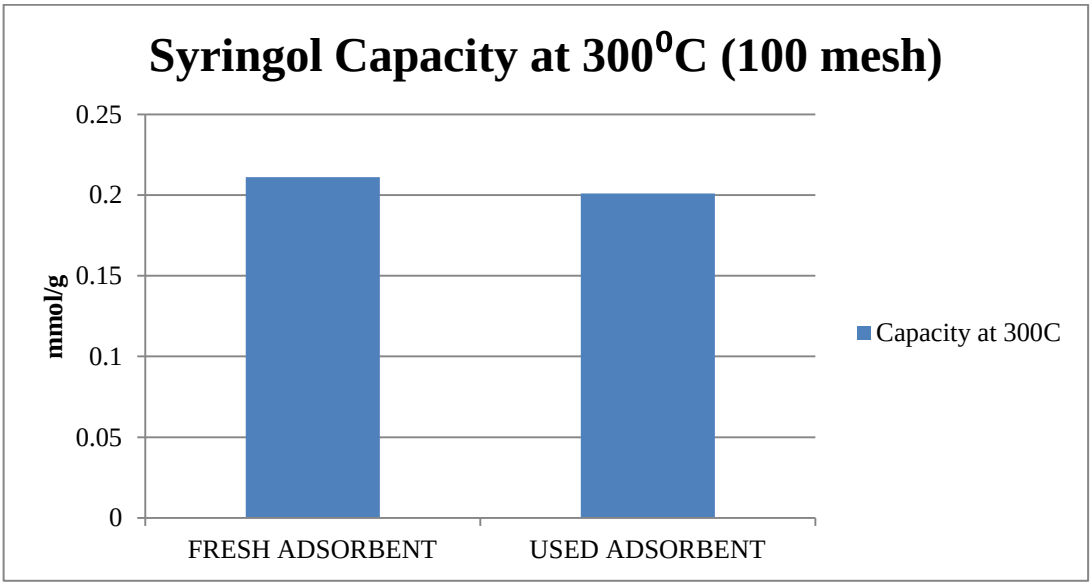

Figure 26: Capacity of syringol over new and used 100 mesh adsorbent at 300 ^{0}C

The capacity change is negligible between the fresh and used adsorbent. The difference could also be contributed to error in the SRI-GC capacity measurement method. This source of error was explained in chapter 3.

In conclusion, a decrease in surface area and pore volume is observed for both sizes of particles of adsorbents tested. The contributor to these decreases would stem

from a decrease in micropore surface area and volume leading to an average pore size larger on a used particle than a fresh particle. The above results would imply that irreversible adsorption is taking place on the activated carbon, specifically in or around the micropores of the adsorbent. The irreversible adsorption analyte would cause the micropores to become covered or filled with coke or char. The coke or char formation would be caused by strongly adsorbing species such as the model methoxyphenolic compounds tested over these adsorbents as explained previously. The larger pores exhibit the same behavior as the micropores, but not to as great extent as the micropores. From the capacity results of syringol over fresh and used adsorbent, it can be seen that negligible capacity is lost from the loss of the micropores of the adsorbent. These results could also correspond to how the 20-40 mesh activated carbon would behave after use and regeneration. This would give evidence that the majority of the adsorption for trapping is occurring in the larger mesopores and macropores after micropores have been covered or filled. The rate of the loss of the micropores is unknown, but as the capacity is unchanged between fresh and used adsorbent the rate of loss is negligible. The number of regenerations of the used adsorbent is approximately 213 times at 300-375 ^{0}C. The capacity results would infer that complete regeneration of the adsorbent is applicable up to approximately 213 cycles of adsorption. There is still a loss of surface area and pore volume for this many cycles, but how much surface area and pore volume need to be lost before capacity is affected is still unknown.

Chapter 5: Mass Spectroscopy of Eluted Model Bio-oil Vapor Components through an Adsorbent Trap

5.1 Experimental and Methodology

The mass spectrometer used in the following experiments is an MKS Microvision Plus Residual Gas Analyzer or RGA. The mass range options that can be scanned for are 1-300 standard atomic mass units (amu). The maximum operating pressure is 7.6*10^-5 Torr and the minimum detectable partial pressure is 1.5*10^-11 Torr. The mass stability is +/-0.1 amu over 8 hours of stable temperature operation. The resolution of the output signal is equal to or greater than ten percent between peaks of equal height. The ion source sensitivity is 2*10^-4 A/mbar. The baseline of the MS was 1*10^-9 Torr during operation, and the vertical axis is a display of partial pressure (Torr) in the mass spectra used for analysis. The computer software used to analyze the results of the MKS instrument is Process Eye 2000. A diagram of the instrument can be seen below in Figure 27:

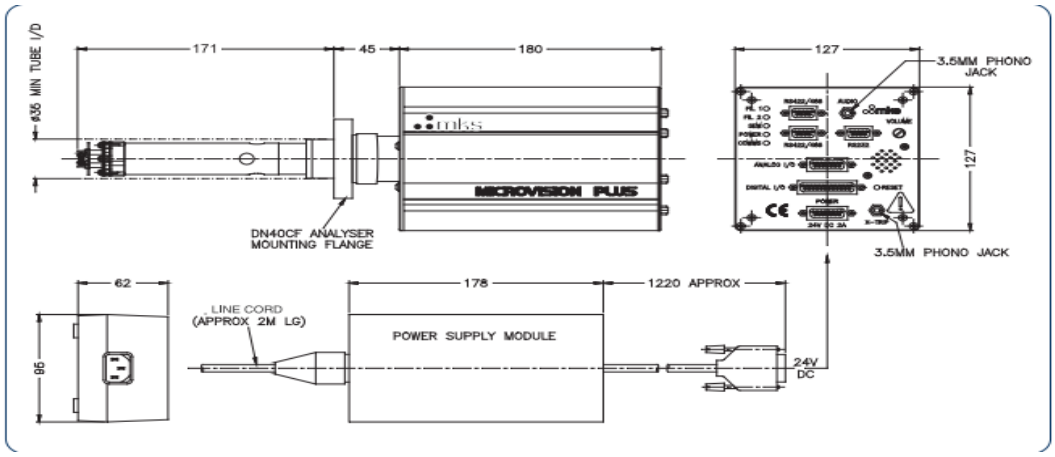

Figure 27: Schematic of the MKS Microvision Plus RGA

The model bio-oil vapor components being used in this study are furan, furfural, acetic acid, and m-cresol. The scanning masses for these compounds are 68, 96, 43, and 108 amu, respectively. These masses were given by the NIST WebBook for the compounds studied.[34] The model compounds were chosen because of their representation of the main compound families found in bio-oil vapors, which are esters, aldehydes, acids, and methoxyphenolic compounds. All chemicals were purchased from Sigma Aldrich and besides the acetic acid, which was in acetone at a concentration of two molar, were injected at pure concentration into the SRI-GC. All injections sizes were 1 µL injections performed with a 10 µL syringe. All injections took place at 300°C to allow desorption from the activated carbon column. The inert carrier for the GC flow through the system was nitrogen at 15 mL/min.

Please refer to chapters two and four for column and adsorbent specifications used in the experiment. The overall configuration of the process flow for an injection of a given component can be seen below in Figure 28:

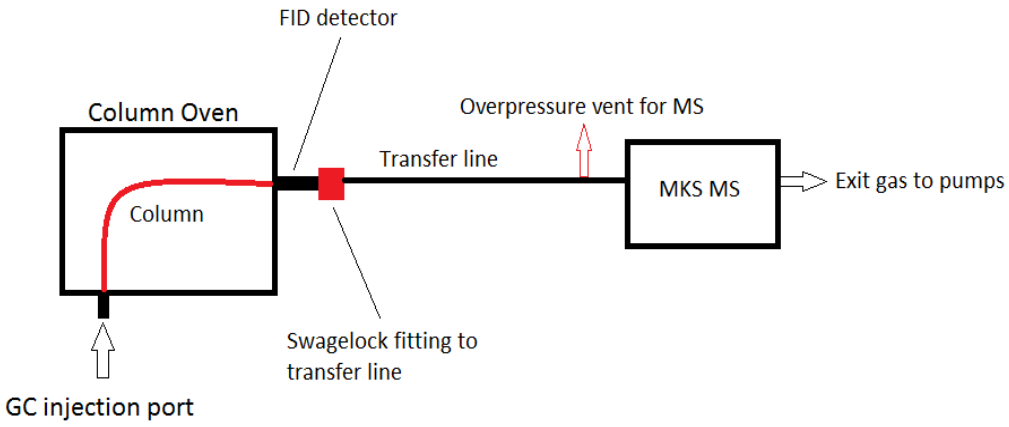

Figure 28: Process flow diagram for GC-MS system

The FID needed to be off during the experiments to prevent ionization of gas sample traveling through the system. The transfer line was heated to 300°C with heating tape to prevent condensation of gases when traveling to the MS. An overpressure vent was used to ensure pressures inside the MS remained at optimum levels during operation.

5.2 Results and Discussion

As noted previously in chapter three, identification is needed of these components to ensure that no secondary or other side reactions are occurring on the surface or active sites of the activated carbon once the components of interest for separation have adsorbed in these places and desorbed back off the column. The model compound adsorption phenomena was studied and the behavior observed was reported in the form of chromatograms analyzed with a mass spectrometer. The first model compound studied to observe if secondary reactions were occurring on the activated carbon trap once an analyte was adsorbed was acetic acid. This compound exhibits very weak adsorptive behavior as indicated by low retention time data, indicative of a weak strength of adsorption. The acetic acid at all temperatures tested in chapters two and three always passes over the adsorbent bed quickly. It can be seen below in Figure 29 by the appearance of the scanned mass of acetic acid (43 amu) that it is the primary component being released through the trap as suspected.

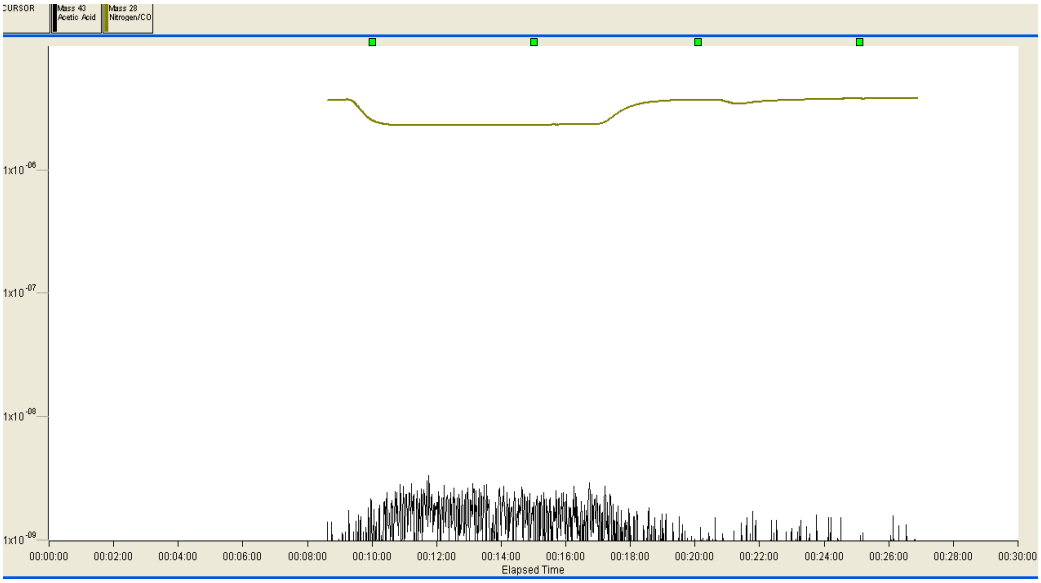

Figure 29: Mass spectrum of desorbed acetic acid from activated carbon

The black trend is the scanned mass of 43 amu which is the mass given by NIST database as acetic acid intensity mass peak. In experiments to be shown, other common by-products of organic reactions were also scanned for, such as carbon dioxide, carbon monoxide, and water. These components were not scanned for in this experiment. In this reaction the orange trend denotes the scanned mass of carbon monoxide/nitrogen which the NIST database reports as 28 amu. It can be seen by Figure 29 that as the acetic acid partial pressure increases the carbon monoxide/nitrogen partial pressure decreases. The behavior is expected as the inert carrier gas used in the SRI instruments GC is nitrogen. By injecting acetic acid and the acetic acid being analyzed by the mass spectrum, the pocket of gas's partial pressure that is carrying the component through the entire system would be decreased as now acetic acid vapors constitute a portion of it.

The next component under analysis is furfural, which, like acetic acid, exhibits low retention times indicative of weak adsorption. The mass scanned for furfural was 96

amu. Carbon dioxide, carbon monoxide, nitrogen, and water given by masses of 44, 28, 28, and 18 amu were also scanned for in this experiment.

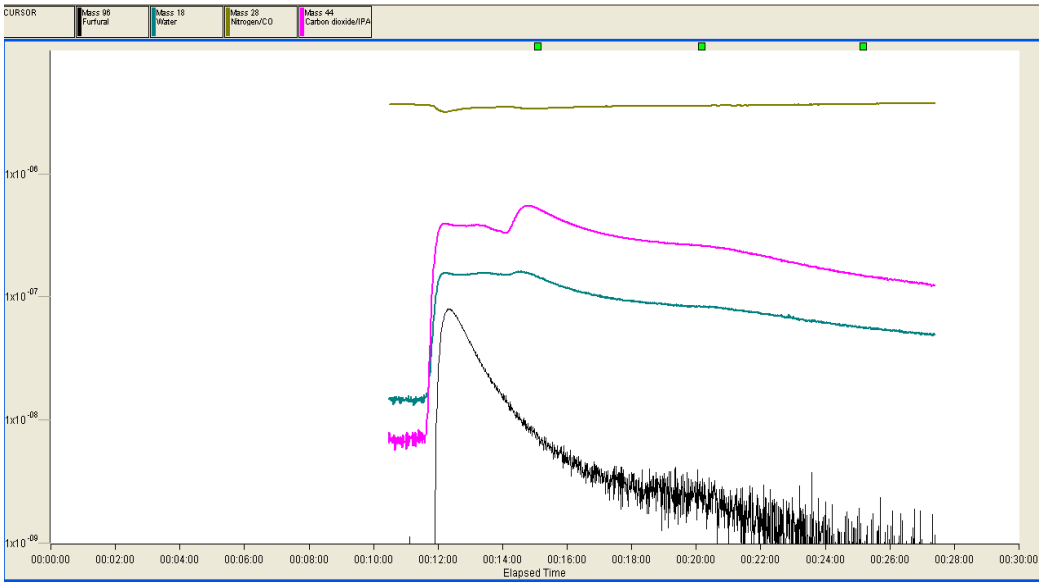

Figure 30: Mass spectrum of desorbed furfural from activated carbon

In Figure 30, it can be observed that furfural is eluting from the activated carbon trap. A slight decrease in the partial pressure of the carrier gas can be seen again, as observed in the acetic acid mass spectrum. As the furfural scanned mass's partial pressure is returning to the baseline, an increase in the partial pressure of carbon dioxide can be seen. According to Malherbe et al., water is a by-product of furfural oligomerization. [35] Furfural oligomerization is most likely occurring because the furfural component is very reactive at high temperatures. The oligmerization reaction could possibly explain the rise in the partial pressure of water. The rise of the partial pressure of carbon dioxide can only be attributed to an ongoing secondary reaction or an injection of gas with the injection of the sample. It is observed the carbon dioxide partial pressure decrease does not decrease proportionately with the furfural decrease in partial pressure. This would imply that the carbon dioxide does not come from a

reaction between furfural and activated carbon because a proportional decrease in partial pressures is not observed for the two components. Overall, besides furfural oligmerization, it is difficult to assume any other secondary reactions from these results.

Furan was studied next and exhibits the same retention time characteristics and therefore strength of bonding over activated carbon as acetic acid and furfural. Masses for water, carbon dioxide, carbon monoxide, and nitrogen were scanned again along with furan. The mass spectra for furan through an activated carbon trap can be seen in Figure 31:

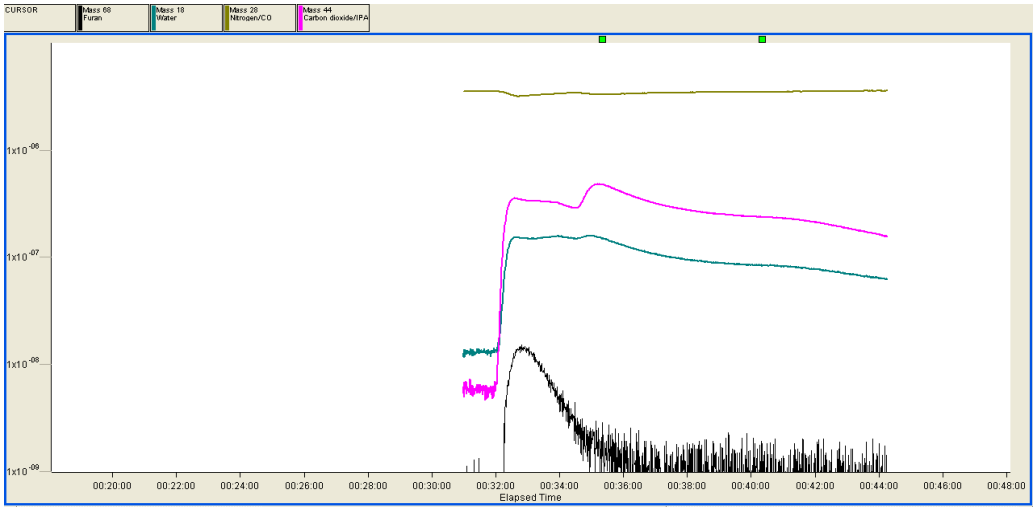

Figure 31: Mass spectrum of desorbed furan from activated carbon

The mass scanned for furan is 68 amu, given by the NIST database. From Figure 31, furan exhibits similar behavior to furfural and acetic acid. According to Nikbin et al., furan can also undergo oligmerization in the presence of electron donating groups.[36] The active sites of the activated carbon can fill this role in the oligomerization of the furan. A by-product of furan oligomerization is water.[36] This would possibly explain the increase in the partial pressure of the water that is occurring once the furan is injected. The same conclusions can be drawn about the increase of

partial pressure of carbon dioxide as in the injection of furfural over activated carbon. Once again, it is difficult to assume any other secondary reactions besides furan oligomerization from the results given.

The last model compound to be analyzed with this method is m-cresol. The mass scanned for in this experiment is 108 amu, provided by the NIST database. Water, carbon monoxide, carbon dioxide, and nitrogen were also scanned for in the experiment. M-cresol as a methoxyphenolic compound exhibits different adsorptive behavior than the previous compounds tested. The methoxyphenolic compounds have the second highest retention times on the activated carbon trap which would be indicative of their stronger adsorption over activated carbon than the other model compounds tested in the retention time studies. As this behavior was noted before, a longer time period had to be waited for the methoxyphenolic compound m-cresol to reach the mass spectrometer. The mass spectrum for m-cresol over an activated carbon trap can be seen in Figure 32:

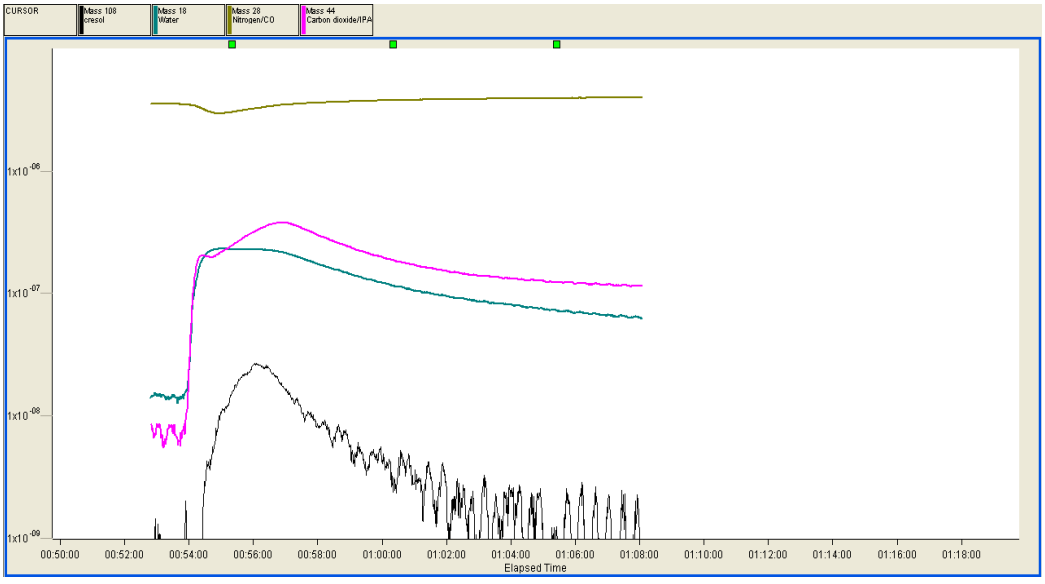

Figure 32: Mass spectrum of desorbed m-cresol from activated carbon

The black trend is the scanned mass of m-cresol and the clear peak shows the initial pulse through the SRI-GC has reached the mass spectrometer. The partial pressures for carbon dioxide and water increase as the injection of cresol is released from the column and travels to the MKS MS. There is currently no research found that has been completed for reactions of m-cresol that produce carbon dioxide and water. The only explainable characteristics of the partial pressure behavior are if the m-cresol is undergoing self-polymerization to produce water and carbon dioxide as by-products. If this assumption were correct, a proportional decrease in the partial pressure of carbon dioxide and water with m-cresol should be observed. This observation is not occurring so a link between the reactant m-cresol and by-products carbon dioxide and water cannot be formulated. From the Figure 32, conclusive evidence is shown that m-cresol eluting from the column but not that secondary reactions are not occurring.

Of the model bio-oil vapor compounds, none show clear evidence of no secondary or side reaction occurring when passing over or adsorbing to the activated carbon trap. All experiments show evidence the component injected over the activated carbon trap is eluting. Whether all the model components are eluting or only a portion of them is still unknown. The behavior of the partial pressures of the carbon dioxide and water for all chromatograms shown is a phenomenon that cannot yet be explained completely. The results of chapter 2 indicate no unexpected products of sizeable amounts for the pyrolysis of biomass over an activated carbon trap. The amount of biomass in these results being pyrolyzed would be too small to say with complete certainty that no secondary reactions are occurring over the trap. If products from secondary reactions were occurring over a trap from pyrolysis vapors, a decrease of the

product amounts found in experiments run without the trap should be observed when run with a trap. The only pyrolysis vapor components that are observed to decrease over a trap considerably are levoglucosan and methoxyphenolics. This is as expected due to trapping of these components. Other components that were not previously seen do not take their place when a trap is implemented, a decrease in the carbon balance is observed from the desired components being trapped. This behavior would be indicative of no secondary reactions occurring with substantial yields.

References

1. Hill, J., et al., *Environmental, economic, and energetic costs and benefits of biodiesel and ethanol biofuels.* Proceedings of the National Academy of Sciences, 2006. **103**(30): p. 11206-11210.

2. Mortensen, P.M., et al., *A review of catalytic upgrading of bio-oil to engine fuels.* Applied Catalysis A: General, 2011. **407**(1): p. 1-19.

3. Zhang, Q., et al., *Review of biomass pyrolysis oil properties and upgrading research.* Energy conversion and management, 2007. **48**(1): p. 87-92.

4. Mohan, D., C.U. Pittman, and P.H. Steele, *Pyrolysis of wood/biomass for bio-oil: a critical review.* Energy & Fuels, 2006. **20**(3): p. 848-889.

5. Czernik, S. and A. Bridgwater, *Overview of applications of biomass fast pyrolysis oil.* Energy & Fuels, 2004. **18**(2): p. 590-598.

6. Rezaei, P.S., H. Shafaghat, and W.M.A.W. Daud, *Aromatic hydrocarbon production by catalytic pyrolysis of palm kernel shell waste using a bifunctional Fe/HBeta catalyst: effect of lignin-derived phenolics on zeolite deactivation.* Green Chemistry, 2016.

7. Pham, T.N., D. Shi, and D.E. Resasco, *Evaluating strategies for catalytic upgrading of pyrolysis oil in liquid phase.* Applied Catalysis B: Environmental, 2014. **145**: p. 10-23.

8. Foster, A.J., et al., *Optimizing the aromatic yield and distribution from catalytic fast pyrolysis of biomass over ZSM-5.* Applied Catalysis A: General, 2012. **423**: p. 154-161.

9. Huber, G.W., S. Iborra, and A. Corma, *Synthesis of transportation fuels from biomass: chemistry, catalysts, and engineering.* Chemical reviews, 2006. **106**(9): p. 4044-4098.

10. Resasco, D.E. and S.P. Crossley, *Implementation of concepts derived from model compound studies in the separation and conversion of bio-oil to fuel.* Catalysis Today, 2014.

11. Yang, H., et al., *Characteristics of hemicellulose, cellulose and lignin pyrolysis.* Fuel, 2007. **86**(12): p. 1781-1788.

12. Du, S., J.A. Valla, and G.M. Bollas, *Characteristics and origin of char and coke from fast and slow, catalytic and thermal pyrolysis of biomass and relevant model compounds.* Green Chemistry, 2013. **15**(11): p. 3214-3229.

13. Jackson, S.D. *Catalyst Deactivation During Pyrolysis Gasoline Hydrogenation*. in *23rd North American Catalysis Society Meeting*. 2013. Nam.

14. Paasikallio, V., et al., *Product quality and catalyst deactivation in a four day catalytic fast pyrolysis production run.* Green Chemistry, 2014. **16**(7): p. 3549-3559.

15. Jae, J., et al., *Investigation into the shape selectivity of zeolite catalysts for biomass conversion.* Journal of Catalysis, 2011. **279**(2): p. 257-268.

16. Mukarakate, C., et al., *Real-time monitoring of the deactivation of HZSM-5 during upgrading of pine pyrolysis vapors.* Green Chemistry, 2014. **16**(3): p. 1444-1461.

17. Shao, S., et al., *Catalytic Pyrolysis of Biomass-Derived Compounds: Coking Kinetics and Formation Network.* Energy & Fuels, 2015. **29**(3): p. 1751-1757.

18. Shoucheng, D., J. Valla, and G.M. Bollas. *Fate of catalyst during catalytic pyrolysis of biomass and relevant model compounds*. in *ABSTRACTS OF PAPERS OF THE AMERICAN CHEMICAL SOCIETY*. 2013. AMER CHEMICAL SOC 1155 16TH ST, NW, WASHINGTON, DC 20036 USA.

19. Díaz, E., et al., *Adsorption characterisation of different volatile organic compounds over alumina, zeolites and activated carbon using inverse gas chromatography.* Journal of chromatography A, 2004. **1049**(1): p. 139-146.

20. Embree, H.D., T. Chen, and G.F. Payne, *Oxygenated aromatic compounds from renewable resources: motivation, opportunities, and adsorptive separations.* Chemical Engineering Journal, 2001. **84**(2): p. 133-147.

21. Dorado, C., C.A. Mullen, and A.A. Boateng, *H-ZSM5 Catalyzed Co-Pyrolysis of Biomass and Plastics.* ACS Sustainable Chemistry & Engineering, 2014. **2**(2): p. 301-311.

22. Zhu, X., et al., *Bifunctional transalkylation and hydrodeoxygenation of anisole over a Pt/HBeta catalyst.* Journal of Catalysis, 2011. **281**(1): p. 21-29.

23. Toh, R.-H., et al., *Immobilized acclimated biomass-powdered activated carbon for the bioregeneration of granular activated carbon loaded with phenol and o-cresol.* Bioresource technology, 2013. **143**: p. 265-274.

24. Žilnik, L.F. and A. Jazbinšek, *Recovery of renewable phenolic fraction from pyrolysis oil.* Separation and Purification Technology, 2012. **86**: p. 157-170.

25. Moreno-Castilla, C., *Adsorption of organic molecules from aqueous solutions on carbon materials.* Carbon, 2004. **42**(1): p. 83-94.

26. Diao, Y., W. Walawender, and L. Fan, *Activated carbons prepared from phosphoric acid activation of grain sorghum.* Bioresource technology, 2002. **81**(1): p. 45-52.

27. Dąbrowski, A., et al., *Adsorption of phenolic compounds by activated carbon—a critical review.* Chemosphere, 2005. **58**(8): p. 1049-1070.

28. Mattson, J.A., et al., *Surface chemistry of active carbon: specific adsorption of phenols.* Journal of Colloid and Interface Science, 1969. **31**(1): p. 116-130.

29. Shirgaonkar, I.Z., et al., *Adsorption equilibrium data for substituted phenols on activated carbon.* Journal of Chemical and Engineering Data, 1992. **37**(2): p. 175-179.

30. Bridgwater, A.V., *Review of fast pyrolysis of biomass and product upgrading.* Biomass and bioenergy, 2012. **38**: p. 68-94.

31. Faix, O., D. Meier, and I. Fortmann, *Thermal degradation products of wood.* Holz als Roh-und Werkstoff, 1990. **48**(7-8): p. 281-285.

32. De Lange, M.F., et al., *Adsorptive characterization of porous solids: Error analysis guides the way.* Microporous and Mesoporous Materials, 2014. **200**: p. 199-215.

33. Leofanti, G., et al., *Surface area and pore texture of catalysts.* Catalysis Today, 1998. **41**(1): p. 207-219.

34. Center, N.M.S.D. and S. Stein, *Mass spectra.* NIST Chemistry WebBook, NIST Standard Reference Database, 2015(69).

35. Roque-Malherbe, R., J. Oñate-Martinez, and E. Navarro, *Furfural oligomerization within H-Fe-FAU zeolite.* Journal of materials science letters, 1993. **12**(13): p. 1037-1038.

36. Nikbin, N., S. Caratzoulas, and D.G. Vlachos, *On the oligomerization mechanism of Brønsted acid-catalyzed conversion of furans to diesel-range fuels.* Applied Catalysis A: General, 2014. **485**: p. 118-122.

Appendix A: Supplementary Figures

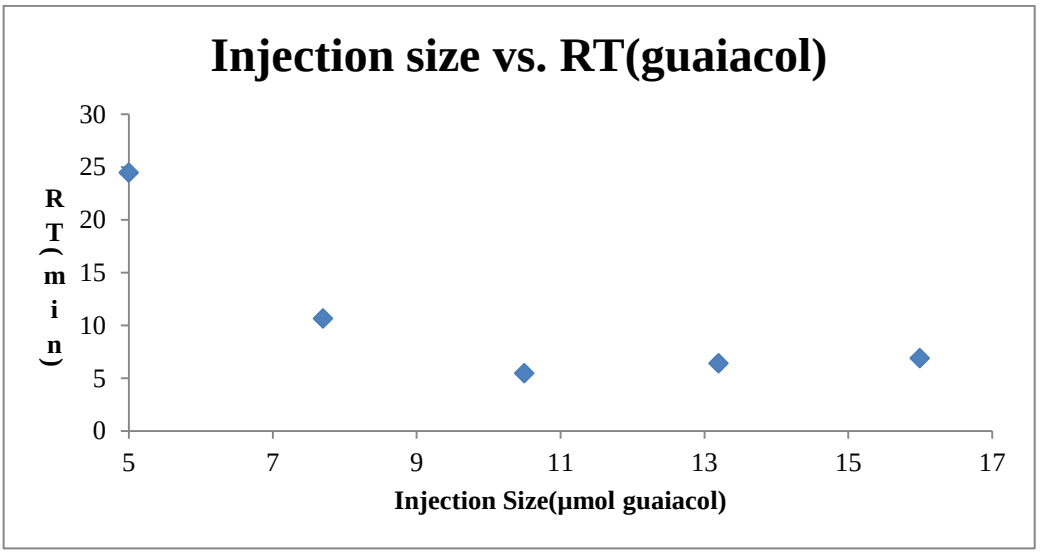

Figure 33:Injection size versus retention time for 2.78 guaiacol/acetone mixture at 300^{0}C (chapter 4)

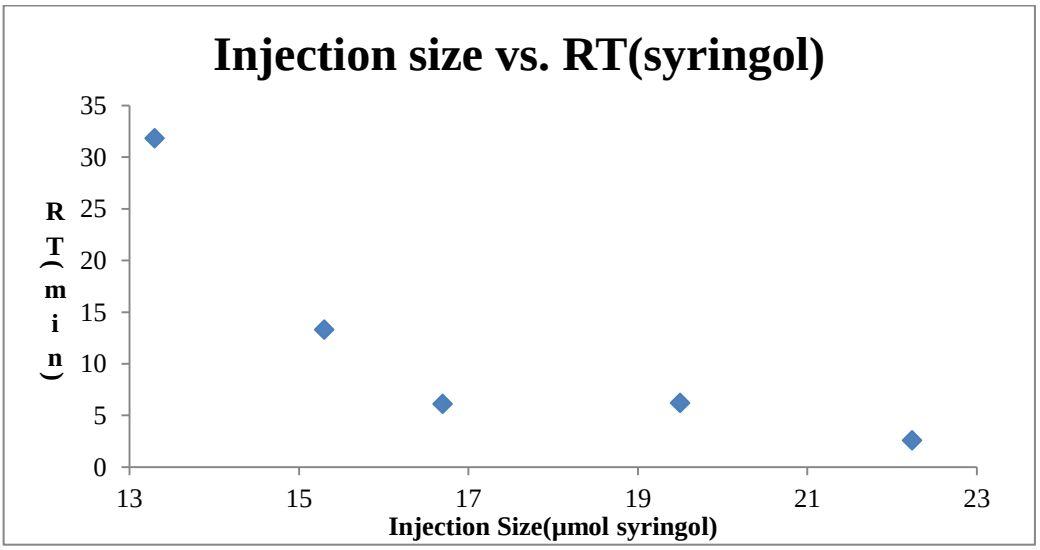

Figure 34: Injection size versus retention time for 2.78 syringol/acetone mixture at 300^{0}C (chapter 4)

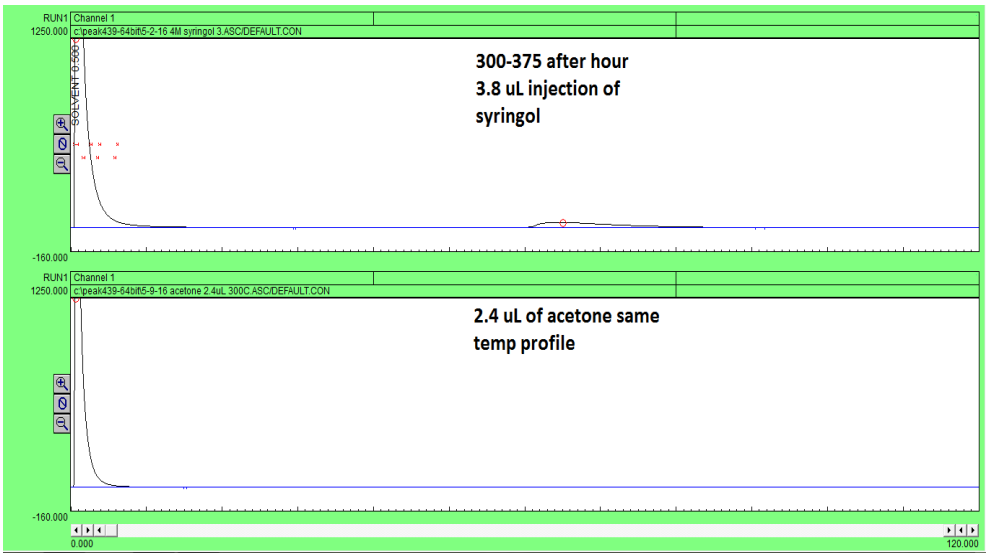

Figure 35: Top chromatogram: injection of 10.56 µmol of syringol at 300^{o}C with bakeout to 375^{o}C after an hour then held for an hour
Bottom chromatogram: injection of pure acetone with same temperature profile

The two chromatograms show a qualitative elution of syringol after an hour after a temperature ramp to 375^{o}C. The beginning injections started at 300^{o}C. The bottom injection shows an injection of pure acetone with same temperature profile as top chromatogram. The two chromatograms show an elution of the trapped syringol on the column if a temperature ramp is used and proves the elution peak is not the acetone. The amount of acetone was injected corresponding to the amount used in the 3.8µl injection of 2.78 M syringol in acetone. This would be supplementary data to chapter 4 proving little to no acetone adsorption.

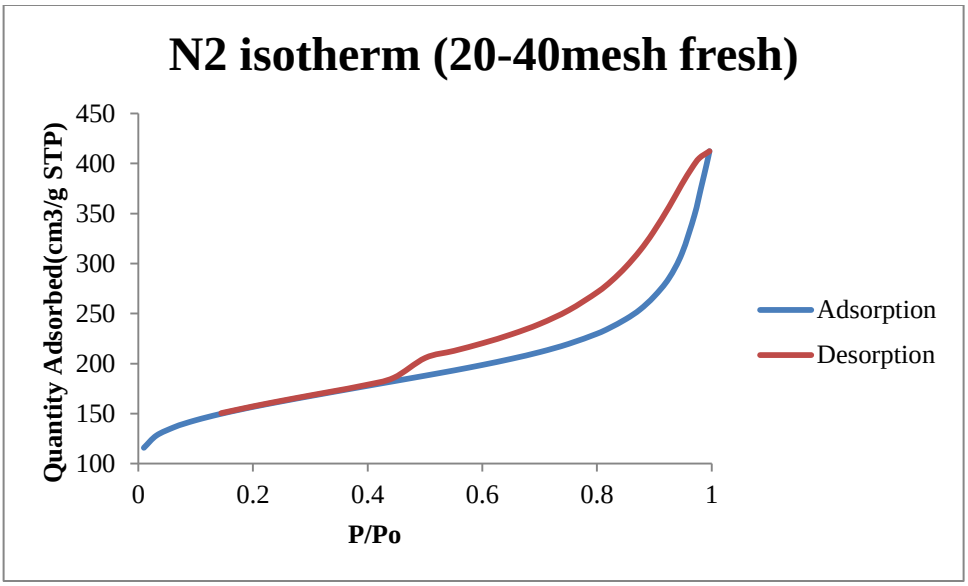

Figure 36: N2 isotherm of 20-40 mesh fresh activated carbon (chapter 5)

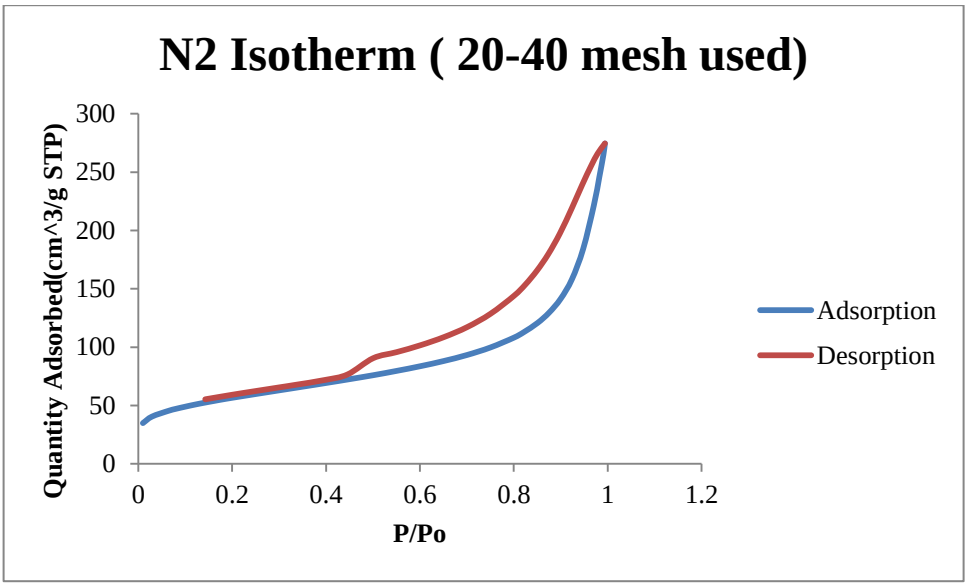

Figure 37: N2 isotherm of 20-40 mesh used activated carbon (chapter 5)

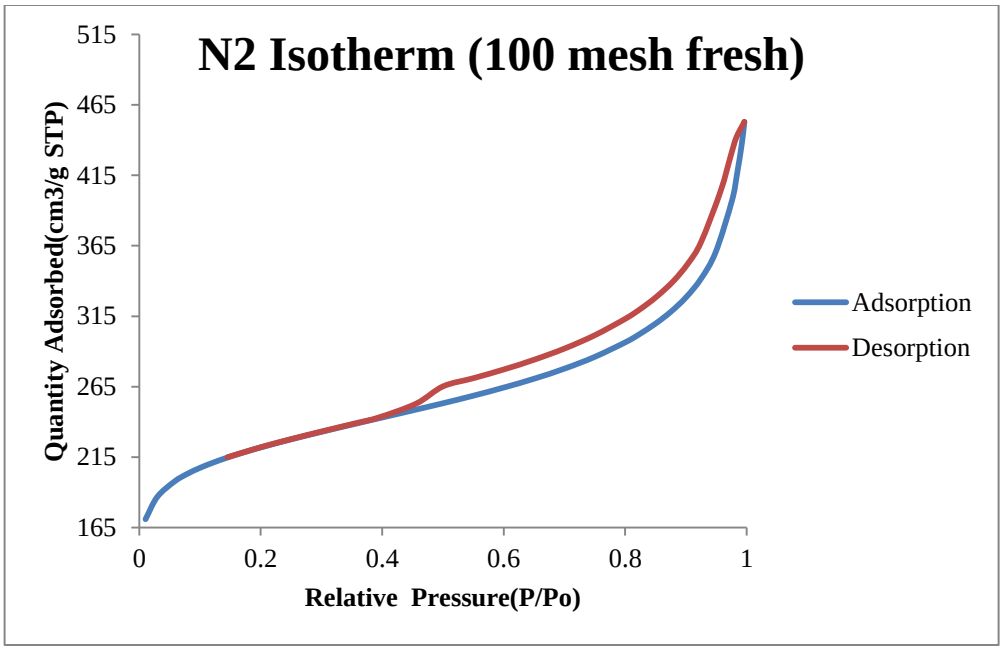

Figure 38: N2 isotherm of 100 mesh fresh activated carbon (chapter 5)

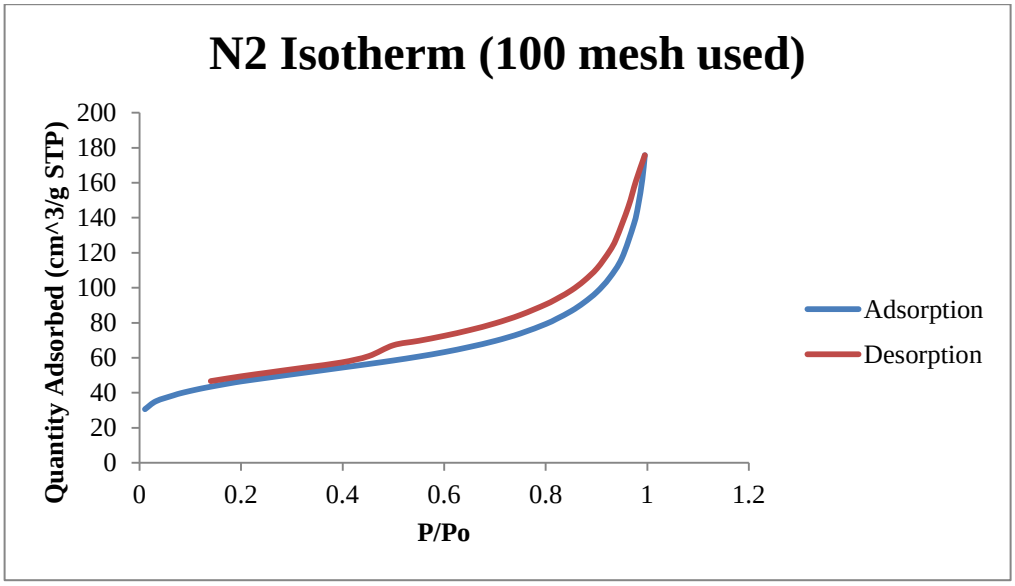

Figure 39: N2 isotherm of 100 mesh used activated carbon (chapter 5)

Appendix B: Sample Calculations

Sample calculation used in chapter 4 to determine amount of activated carbon to remove all methoxyphenolics from 1000 tons of biomass pyrolysis streams per day.

Assumptions: 25% yield to liquid products from solid pyrolysis

5% of liquid is methoxyphenolic compounds

0.2mmol/g capacity for methoxyphenolic compounds over activated carbon

300°C adsorbent bed

Minimal adsorption of compounds that is undesired to trap

Regeneration of bed within 1 hour

Average molecular weight of methoxyphenolic compounds is 154 g/mol

Methoxyphenolic compounds in stream per hour is 0.52 tons

Uniform production of components from pyrolysis of biomass

$$\frac{1000\ tons\ biomass}{day} * 0.25\ yield\ to\ liquid\ products$$

$$* 0.05\ methoxyphenolics\ liquid * \frac{2000\ lbs}{1\ ton} * \frac{1\ kg}{2.2\ lbs} * \frac{1000\ g}{1\ kg}$$

$$* \frac{mol\ methoxyphenolics}{154\ g} * \frac{g\ activated\ carbon}{0.2\ mmols} * \frac{1000\ mmol}{mol}$$

$$* \frac{1\ kg}{1000\ g} * \frac{2.2\ lbs}{1\ kg} * \frac{1\ ton}{2000\ lbs} = \frac{405.84\ tons\ of\ activated\ carbon}{day}$$

$$\frac{405.84\ tons\ of\ activated\ carboni}{day} * \frac{day}{24\ hours} = \frac{16.9\ tons\ of\ activated\ carbon}{hr}$$

Two separate beds composed of 16.9 tons of activated carbon. This would be a total of 33.8 tons of activated carbon. Adsorption taking place over an hour and regeneration taking place over an hour. Depiction of system seen below.

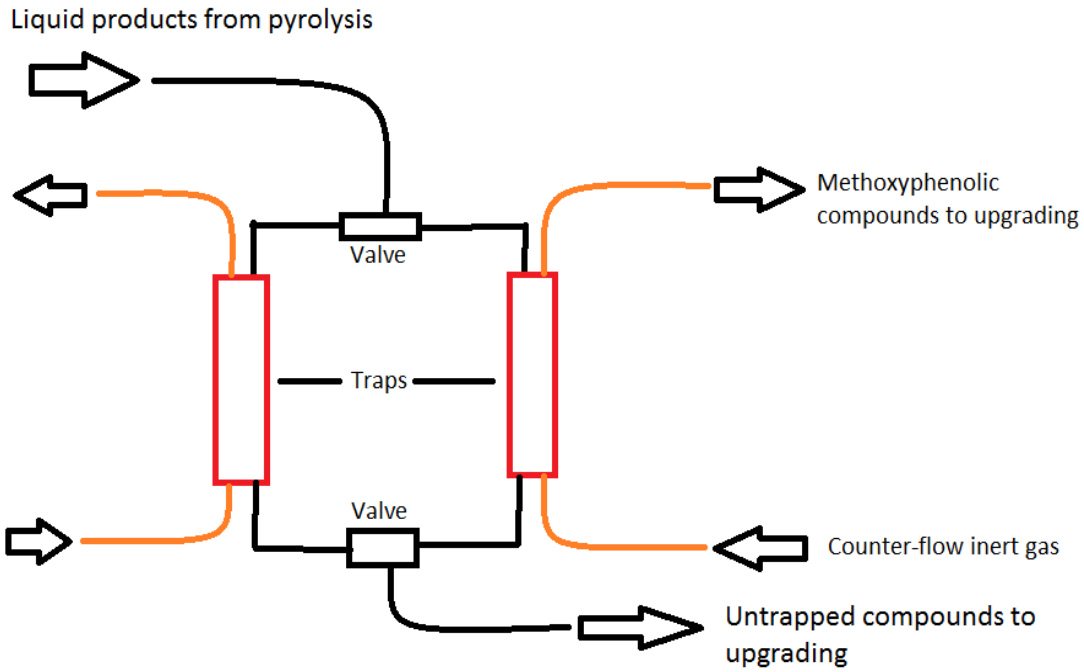

Figure 40: Simulated moving bed system for trapping of methoxyphenolics compounds from pyrolysis products

Maximum amount of syringol activated carbon could hold from pore volume

Assumptions: Pore volume is 0.53 cm^3/g

Density of syringol is 1.1 g/cm^3

Molecuar weight of syringol is 154 g/mol

$$\frac{0.53\ cm^3}{g} * \frac{1.1\ g}{cm^3 syringol} * \frac{mol\ syringol}{154\ g} * \frac{1000\ mmol}{1\ mol} = 3.7\ \frac{mmol}{g}$$